



**UNIVERSIDAD DE INVESTIGACIÓN DE
TECNOLOGÍA EXPERIMENTAL YACHAY**

Escuela de Ciencias Biológicas e Ingeniería

**TÍTULO: Analysis of Intracorporeal
Communication Channels from 100 KHz to 200
MHz: Experimental Transmission Characteristics**

**Trabajo de integración curricular presentado como requisito para la
obtención del título de Ingeniero Biomédica**

AUTOR

Michelle Camila Muñoz Guerrero

TUTOR

PhD. Diego Alfonso Almeida

SECRETARÍA GENERAL
ESCUELA DE CIENCIAS BIOLÓGICAS E INGENIERÍA
CARRERA DE BIOMEDICINA
ACTA DE DEFENSA No. UITEY-BIO-2022-00031-AD

En la ciudad de San Miguel de Urcuquí, Provincia de Imbabura, a los 11 días del mes de octubre de 2022, a las 11:00 horas, en el Aula VIRTUA de la Universidad de Investigación de Tecnología Experimental Yachay y ante el Tribunal Calificador, integrado por los docentes:

Presidente Tribunal de Defensa	Mgs. VILLALBA MENESES, GANDHI FERNANDO
Miembro No Tutor	CRUZ VARELA, JONATHAN DAVID
Tutor	Dr. ALMEIDA GALARRAGA, DIEGO ALFONSO , Ph.D.

Se presenta el(la) señor(ita) estudiante **MUÑOZ GUERRERO, MICHELLE CAMILA**, con cédula de identidad No. **0105700710**, de la **ESCUELA DE CIENCIAS BIOLÓGICAS E INGENIERÍA**, de la Carrera de **BIOMEDICINA**, aprobada por el Consejo de Educación Superior (CES), mediante Resolución **RPC-SO-43-No.496-2014**, con el objeto de rendir la sustentación de su trabajo de titulación denominado: **Analysis of Intracorporeal Communication Channels from 100 KHz to 200 MHz: Experimental Transmission Characteristics**, previa a la obtención del título de **INGENIERO/A BIOMÉDICO/A**.

El citado trabajo de titulación, fue debidamente aprobado por el(los) docente(s):

Tutor	Dr. ALMEIDA GALARRAGA, DIEGO ALFONSO , Ph.D.
--------------	--

Y recibió las observaciones de los otros miembros del Tribunal Calificador, las mismas que han sido incorporadas por el(la) estudiante.

Previamente cumplidos los requisitos legales y reglamentarios, el trabajo de titulación fue sustentado por el(la) estudiante y examinado por los miembros del Tribunal Calificador. Escuchada la sustentación del trabajo de titulación, que integró la exposición de el(la) estudiante sobre el contenido de la misma y las preguntas formuladas por los miembros del Tribunal, se califica la sustentación del trabajo de titulación con las siguientes calificaciones:

Tipo	Docente	Calificación
Presidente Tribunal De Defensa	Mgs. VILLALBA MENESES, GANDHI FERNANDO	10,0
Miembro Tribunal De Defensa	CRUZ VARELA, JONATHAN DAVID	10,0
Tutor	Dr. ALMEIDA GALARRAGA, DIEGO ALFONSO , Ph.D.	10,0

Lo que da un promedio de: **10 (Diez punto Cero)**, sobre 10 (diez), equivalente a: **APROBADO**

Para constancia de lo actuado, firman los miembros del Tribunal Calificador, el/la estudiante y el/la secretario ad-hoc.

MUÑOZ GUERRERO, MICHELLE CAMILA

Estudiante



Firmado electrónicamente por:
GANDHI FERNANDO
VILLALBA MENESES

Mgs. VILLALBA MENESES, GANDHI FERNANDO

Presidente Tribunal de Defensa

DIEGO ALFONSO
 ALMEIDA
 GALARRAGA

Firmado digitalmente por
 DIEGO ALFONSO ALMEIDA
 GALARRAGA
 Fecha: 2022.10.11 12:05:27
 -05'00'

Dr. ALMEIDA GALARRAGA, DIEGO ALFONSO , Ph.D.

Tutor



Firmado electrónicamente por:
JONATHAN
DAVID CRUZ
VARELA

CRUZ VARELA, JONATHAN DAVID

Miembro No Tutor



Firmado electrónicamente por:

**KARLA
ESTEFANIA
ALARCON FELIX**

ALARCON FELIX, KARLA ESTEFANIA
Secretario Ad-hoc

AUTORÍA

Yo, **Michelle Camila Muñoz Guerrero** pop-con cédula de identidad 0105700710, declaro que las ideas, juicios, valoraciones, interpretaciones, consultas bibliográficas, definiciones y conceptualizaciones expuestas en el presente trabajo, así como los procedimientos y herramientas utilizadas en la investigación, son de absoluta responsabilidad de la autora del trabajo de integración curricular. Así mismo, me acojo a los reglamentos internos de la Universidad de Investigación de Tecnología Experimental Yachay.

Urcuquí, febrero 2022

Michelle Camila Muñoz Guerrero

CI. 0105700710

AUTORIZACIÓN DE PUBLICACION

Yo, **Michelle Camila Muñoz Guerrero** con cédula de identidad 0105700710, cedo a la Universidad de Investigación de Tecnología Experimental Yachay, los derechos de publicación de la presente obra, sin que deba haber un reconocimiento económico por este concepto. Declaro además que el texto del presente trabajo de titulación no podrá ser cedido a ninguna empresa editorial para su publicación u otros fines, sin contar previamente con la autorización escrita de la Universidad.

Asimismo, autorizo a la Universidad para que realice la digitalización y publicación de este trabajo de integración curricular en el repositorio virtual, de conformidad a lo dispuesto en el Art. 144 de la Ley Orgánica de Educación Superior.

Urcuquí, febrero 2022

Michelle Camila Muñoz Guerrero

CI. 0105700710

Dedictory

A Miriam, Nicole, Juliana y Fabian, mi familia por apoyarme y alentarme a tomar riesgos y sin importar en que parte del mundo este se que puedo volver a mi hogar. A ustedes les dedico todo el esfuerzo que puse en mi vida Universitaria.

Acknowledgments

I would like to acknowledge to my advisor Dr. Diego Almeida for his support, guide, motivation and continuous recommendations for the development of this project. I thank his for always be willing to receive my doubts and propose ideas for this study without his guidance and tenacity, this dissertation would not have been possible.

Very special gratitude to my parents who support me unconditionally, their confidence in my capacities and for always trust in me and my dreams and thanks to my university friends who were my second family and encouraged me when I spent difficult moments.

Finally, I would thank the King Abdullah University of Science and Technology (KAUST) and the Smart Health Initiative (SHI) at KAUST for the financial support for this work.

Resumen

Recientemente los Sistemas de Comunicación Humana ha surgido como una nueva tecnología en la vida cotidiana pero con especial importancia en la medicina. Este sistema de comunicación conecta dispositivos de potencia ultrabaja en el cuerpo humano (dispositivos portátiles o dispositivos implantables) para prevenir, diagnosticar o controlar enfermedades. En este nuevo sistema de comunicación, el cuerpo humano se comporta como un medio que conecta el transmisor y el receptor, que se colocan directamente sobre la piel o están en su proximidad, es decir, la ruta de transmisión de la señal se cerrará a través del cuerpo humano y la ruta de la señal de retorno se cerrará capacitivamente a través del entorno. En HBC el nivel de la señal recibida se ve afectada por diferentes factores, que afectan al transmisor y receptor. Para estudiar el efecto de esto se fabricó diferentes tipos de electrodos de cobre variando la forma, orientación y configuración de estos. Después se eligió el electrodo con menos pérdida de señal. A este electrodo se evaluó en diferentes medios usados comúnmente en HBC como son sal con agua, gelatina y brazo humano. Estos resultados experimentales muestran que junto con la dependencia de la frecuencia la señal transmitida es afectada dependiendo la configuración de los electrodos transmisor y receptor.

Palabras Claves: Comunicaciones del cuerpo humano, electrodos, acoplamiento galvánico, acoplamiento capacitivo

Abstract

Recently, Human Communication Systems have emerged as a new technology in daily life but with special importance in medicine. This communication system connects ultra-low power devices in the human body (wearable devices or implantable devices) to prevent, diagnose or control diseases. . In this new communication system, the human body behaves as a medium connecting the transmitter and the receiver, which are placed directly on the skin or in its proximity, that is, the signal transmission path will be closed through of the human body and the return signal path will be capacitively closed through the environment. In HBC the received signal level is affected by different factors, which worsen the transmitter and receiver. To study the effect of this, different types of copper electrodes were manufactured, varying their shape, orientation and configuration. Then the appliance with less signal loss was chosen. This appliance is evaluated in different media commonly used in HBC such as salt with water, gelatin, and human arm. These experimental results show that along with the frequency dependency the transmitting signal is affected depending on the configuration of the transmitting and receiving electrodes.

Key Words: Human body communications, Electrodes, Galvanic Coupling, Capacitive Coupling

Contents

Contents	7
List of Figures	10
List of Tables	12
1 Introduction	1
1.1 Problem Situation	1
1.2 Problem Statement	2
1.3 Justification	2
1.4 Scope	3
1.5 Thesis Overview	5
2 Objectives	6
2.1 General objective	6
2.2 Specific objectives	6
3 State of Art	7
3.1 Body Area networks	7
3.2 Wireless Body Area Network technologies	8
3.2.1 IEEE 802.15.1 (Bluetooth)	8
3.2.2 Ultra-Wideband-IEEE 802.15.3	10
3.2.3 ZigBee-IEEE 802.15.4	11
3.2.4 WiFi – IEEE 802.11	11
3.3 Applications of Wireless Body Area Network	12
3.4 Human Body Chanel	15
3.5 Parameters and Electric Properties	16
3.5.1 Dielectric properties of a human body	16
3.5.2 Path loss	18
3.6 HBC Transmission Systems	19
3.6.1 Capacitive Coupling Body Transmission	19

3.6.2	Galvanic Coupling Body Transmission	20
3.7	Two-Port Network Theory	21
3.7.1	Scattering Parameters	21
3.7.2	Z Parameters	23
3.7.3	Transmission Lines: Reflection Coefficient, VSWR and Power Transmitted	24
4	Materials and Methodology	28
4.1	Equipment and Calibration	28
4.2	Phantom building	31
4.2.1	Salty water medium	31
4.2.2	Gelatin Medium	32
4.2.3	Human Arm	33
4.3	Electrodes Fabrication	34
4.3.1	Square electrodes	35
4.3.2	Circular electrodes	35
4.3.3	Planar Capacitive Electrodes	36
4.3.4	Planar Galvanic Electrodes	37
4.4	ANALYSIS	37
4.4.1	SWR	37
4.4.2	POWER TRANSMITTED	38
5	Results and Discussions	39
5.1	Results of Transmission data using different configuration of electrodes	39
5.1.1	Results of Square Electrodes	39
5.1.2	Results of Circle electrodes	41
5.1.3	Results of Planar Capacitive Electrodes	43
5.1.4	Results of Planar Galvanic Electrodes	45
5.2	Discusions	46
5.3	Results of Transmission data through mediums	48
5.3.1	Return Loss	49
5.3.2	Impedance	50

5.3.3	SWR	51
5.3.4	Power Transmitted	53
5.4	Discussions	55
6	Conclusions	57
7	Future Perspectives	57
8	References	58
	References	58

List of Figures

2	WBAN common architecture consists of three tiers of communications: a)Intra-BAN communications, b)Inter-BAN communications and c) beyond- BAN communications	8
3	Bluetooth Architecture	9
4	Block of scheme of the UWB medical scenario	10
5	Applications of WBAN	15
6	Measurements of the relative permittivity of Dry Skin by Gabriel and Gestblom [1]	17
7	Measurement of the conductivity (S/m) of Dry Skin by Gabriel and Gestblom [1]	18
8	Capacitive Coupling HBC	20
9	Galvanic Coupling HBC	20
10	Two port network	22
11	reflection	24
12	Reflection	27
13	Setup to measure by using a VNA	29
14	mini vna calibration pro using SOLT	30
15	Calibration Kit SOLT	30
16	Calibration in progress	30
17	Calibration done for 4 S-Parameters	30
18	Software created in Labview	31
19	General View	31
20	Test	31
21	liquid samples	32
22	Gelatin samples	33
23	Experimental setup for Capacitive and Galvanic Coupling on a human arm, showing the current paths on human's body.	34
24	Insulator Material	34
25	Square electrodes 2x2 cm	35
26	Circular electrodes 2x2 cm	36

27	Planar Capacitive electrodes 2.5 cm of diameter.	36
28	Planar Galvanic electrodes 2.5 cm of diameter.	37
29	Experimental characterization of planar capacitive electrode at 15 cm .	39
30	Capacitive Square axial electrodes. Return Loss (S_{11}) (a), Return Phase (b), Impedance modulus $ Z $ (c) and Nyquist Plot (d)	41
31	Circular Axis Electrodes electrodes for different separations.Return Loss (S_{11}) (a), Return Phase (b), Impedance modulus $ Z $ (c) and Nyquist Plot (d)	43
32	Planar Capacitive electrodes for different separations.Return Loss (S_{11}) (a), Return Phase (b), Impedance modulus $ Z $ (c) and Nyquist Plot (d)	44
33	Planar Galvanic electrodes for different separations.Return Loss (S_{11}) (a), Return Phase (b), Impedance modulus $ Z $ (c) and Nyquist Plot (d)	46
34	Experimental characterization of circular electrodes through Human Arm	49
35	Channel characterization of the CC circular electrodes with axial excitation for different distances and media. Liquid medium return loss (a), Gel medium return loss (b) and measurement on subject's arm of the return loss (c)	50
36	Channel characterization of the CC circular electrodes with axial excitation for different distances and media. Liquid medium of $ Z $ (a),Gel medium of $ Z $ (b), and measurement on subject's arm of $ Z $ (c)	51
37	Channel characterization of the CC circular electrodes with axial excitation for different distances and media. Liquid medium of SWR (a),Gel medium of SWR (b), and measurement on subject's arm of SWR (c) .	53
38	Channel characterization of the CC circular electrodes with axial excitation for different distances and media. Liquid medium of % Power Transmitted (a),Gel medium of % of Power Transmitted (b), and measurement on subject's arm of % of Power Transmitted (c)	54

List of Tables

1	Characteristics Wireless Body Area Network technologies	12
2	Different WBAN application	14
3	Reference levels for current induced in any limb, averaged over 6 min, at frequencies from 100 kHz to 110 MHz.	16
4	Measurements of electrodes with VNA in diferents mediums	28
5	Composition of Salty Water Samples.	32
6	Gelatin Fabrication	33
7	Measurements of electrodes with VNA in diferents mediums	38
8	Measurements of electrodes with VNA	48
9	Measurements of electrodes with VNA in diferents mediums	56

List of Equations

Ec.1 Electric field Strength	17
Ec.2 Input voltage reflection	22
Ec.3 Reverse voltage gain	22
?? Forward voltage gain	22
Ec.5 Output voltage reflection	22
Ec.6 Open-circuit conditions	23
Ec.7 Z parameters of a two port network	23
Ec.8 Input driving point Impedance	23
Ec.9 Forward transfer Impedance	23
Ec.10 Reverse transfer Impedance	24
Ec.11 Output driving point Impedance	24
?? Forward voltage gain	24

Abbreviations

BAN: Body Area Networking.

BLE: Bluetooth Low Energy .

CC: Capacitive Coupling.

CVD: Cardiovascular disease.

DI: Deionized.

GC: Galvanic Coupling.

IBC: Intra Body Communications.

ICNIRP:International Commission on Non-Ionizing Radiation Protection

IEEE: The Institute of Electrical and Electronics Engineers

INEC: National Institute of Statistics and Censuses.

IoT:Internet of things.

ISM:Industrial, Scientific and Medical band.

EKG: Electrocardiogram.

EMC:Electromagnetic compatibility.

GHz: Gigahertz.

Kpbs: Kilobit per second.

LPWAN: Low-power wide-area network.

Mbps: Megabit per second.

MHz: Megahertz.

NCDs: Non-communicable diseases.

NIOSH: National Institute for Occupational Safety and Health

PAHO: Pan American Health Organization.

PD: Parkinson's disease.

PDA: Personal digital assistant.

PANs: Personal area networks.

RX: Receiver.

TX: Transmitter

UWB: Ultra-wideband.

VNA: Vector Network Analyzer.

WBAN: Wireless Body area networks.

WLAN: wireless local-area network

WHO: World Health Organization's global.

1. Introduction

1.1. Problem Situation

Aging of the population is a global phenomenon. The elderly population aged 65 and above numbered 500 million in 2006 [2]. By 2030, the number will be almost doubled to around 1 billion. While global aging represents a triumph of medical, social and economic advances over disease, it also presents tremendous challenges to the society and healthcare systems all over the world. The proportion of deaths due to age-related chronic diseases is projected to rise from 59% in 2002 to 69% in 2030 [3]. If not carefully prevented and managed, chronic diseases will become the most expensive financial burden on our society. For example, it is anticipated that China will lose \$558 billion in foregone national income over the next ten years due to premature deaths caused by heart disease, stroke and diabetes, according to the World Health Organization's global(WHO) report in 2005[4] .

The growing aging population, skyrocketing healthcare costs, and prevalence of chronic diseases are the main driving forces to propel the fundamental transformation of the current healthcare systems [5]. Health providers are looking for more cost-effective and responsive ways to deliver healthcare services[6]. The conventional hospital-centered healthcare system, which focuses on diagnosis and treatment, is shifting its focus towards an individual-centered healthcare system with emphasis on early detection of risk factors, early diagnosis, and early treatment [7],[8]and [9]

The new paradigm of p-Health aims to encourage the participation of the whole nation in the prevention of illnesses or early prediction of diseases such that pre-emptive treatment can be delivered thus achieving a pervasive and personalized healthcare [2]. In this paradigm shift, wearable medical systems have been recognized as an enabling technology for monitoring a individual's health condition on a continuous basis, feeding relevant information back to the users and/or medical professionals, and firing an alarm signal when an adverse condition occurs [7], [10], [11]

1.2. Problem Statement

Non-communicable diseases (NCDs) are long-term conditions that evolve and generate high rates of morbidity and mortality, affecting the well-being individual and family. They are the leading cause of overall mortality and preventable premature death in the Americas and Ecuador. Their burden affects socioeconomic development and represents a financial burden for the health sector. The NCDs prioritized by the Pan American Health Organization/World Health Organization Health (PAHO/WHO) are cardiovascular diseases, diabetes mellitus, cancer, and chronic respiratory diseases. These are related to the biological RFs: overweight and obesity, high blood pressure, high blood glucose, and high blood cholesterol. The prevalence of these RF in the Americas is high in the global context.

In Ecuador, according to data from the National Institute of Statistics and Censuses (INEC), in 2018 the NCDs represented 53% of all deaths. Of these, 48.6% corresponded to cardiovascular disease (CVD), 30% to cancer, 12.4% to diabetes and 8.7% to chronic respiratory diseases [12]. Besides, In our country there are: 1,049,824 people over 65 years of age (6.5% of the total population). The Government of the Citizen Revolution implements public policies based on the defense of rights and recognition of the value of the population older adult, whose participation is progressively determined. By 2054, they are expected to represent 18% of the population. For women, life expectancy will be higher at 83.5 years compared to 77.6 years for men. The Ecuadorian State recognizes older adults as holders of rights, as enshrined in our Constitution in articles 36, 37 and 38. Free and specialized health care.

1.3. Justification

Human Body Communication has multiple advantages in comparison with traditional radio frequency (RF) communication. First, it alleviates the traffic load from the radio channels, which are becoming more and more congested, as the number of connected wireless devices increases rapidly [13]. Nearby RF devices operating at the same band cause interference and co-existence issues. This is an incredibly challenging issue, especially for the Industrial, Scientific and Medical band that rapidly becomes

saturated and interference-limited by the ever increasing number of Internet of things (IoT) devices.

Second, RF makes the privacy and confidentiality of sensitive data susceptible to overhearing, eavesdropping, bio-hacking, and interception. Since system complexity and monetary cost increase with additional security measures, which negatively impact SWaP-C constraints, it is better to use communication methods with inherent physical layer security features. Body channels can potentially provide higher security than traditional RF communication since the electric field stays in the vicinity of a human body. The signal is confined to the surface of the body and with little energy radiated into the surrounding environment (avoid the body acting as antenna to radiate energy) [14] , [15]. Therefore, the security of information is guaranteed for its avoidance of eavesdropping, and the interference among different individuals can be minimized as well [16].

The radio front-end is one of the most complex and power-hungry sub-systems of RF devices, which increases the battery size and causes violation of the Size, Weight, Power and Cost constraints. The resulting form-factors and frequent charging requirements naturally decrease quality of experience and commercialization success. Low Signal Attenuation-Low Transmission Power compared with air channel, human body channel obtains high channel gain [17], which can lower the transmission power and thus it may potentially lower the power consumption of the system and helpful for miniaturization.

1.4. Scope

The contributions of this paper are summarized in the following points;

- Fabricate four copper electrodes for capacitive and galvanic coupling for intra-body communication.
- The fabricated electrodes are tested and measured on three different media including: Liquid medium, gel medium and skin.

- The fabricated electrodes are tested and measured for three different distances between the TX and Rx: 4, 10 and 15 cm.
- The fabricated electrodes are characterized to obtain, Return Loss, Modulus Impedance Nyquist plot be to identify the optimum frequency range for HBC.

1.5. Thesis Overview

The advancement of aging globally represents a challenge in society. By 2054, life expectancy for women is expected to exceed 83.5 years and for men 77.6 years. In Ecuador, according to the Inc, in 2018 there were 53 deaths from diseases such as cancer, diabetes, respiratory diseases, these diseases are very common in adulthood and, since they are not treated, they become the most expensive financial burden. For this reason, there are many studies where health is focused on new cost-effective ways of diagnosis, treatment, and personalized medical care. Given this, today we have portable medical systems with the latest Human Body Communication technology.

Communication systems in the human body relieve the traffic load from radio channels, which become increasingly congested as the number of connected wireless devices rapidly increases [13] limited by the ever-increasing number of Internet devices of things (IoT). Second, RF makes the privacy and confidentiality of sensitive data susceptible to eavesdropping, eavesdropping, biopiracy, and interception, since the electric field remains close to the human body. Therefore, the security of information is guaranteed and the interference between different individuals. can also be minimized [16]. And thus it can potentially reduce system power consumption and be useful for miniaturization

2. Objectives

2.1. General objective

Study the effect of the level received signal with different types of copper electrodes, which were manufactured by varying their shape and orientation. Then the electrode with less signal loss was evaluated in different media commonly used in Human Body communication.

2.2. Specific objectives

- Identify the optimum frequency range for HBC to design better interface circuits with the human body channel to minimize total loss, thus minimizing the power needed for transmission.
- Identify influence of different parameters on HBC such as type, shape, and size of the electrodes using different distance between the transmitter and the receiver.
- Identify influence of different mediums using on HBC such as salty water, gelatin and human arm.

3. State of Art

3.1. Body Area networks

In recent years, with the continuous improvement of living quality, people pay more attention to their own health care so the medical model of diagnosis and prevention has gradually entered people's daily life. In the community and family, people can monitor their physical indices more synthetically anytime or anywhere. That is possible through a series of small intelligent wearable or implantable health care devices. Therefore real-time monitoring of patients and remote medical clinical diagnostics are going to be a crucial part of the healthcare system. In this context, Wireless Body area networks (WBAN) initially proposed by Zimmerman [18], constitute an active field of research and development. It offers the potential of great improvement in the delivery and monitoring of healthcare. This emerging technology promises increases in efficiency, accuracy and availability of medical treatment due to the recent advances in wireless communication and in electronics offering small and intelligent sensors able to be used in the human body.

WBANs consists of a number of heterogeneous biological sensors. which are placed in or around the human body. Through these sensors, real-time monitoring could be implemented remotely. Each of them has specific requirements and is used for different missions. For example, an EEG sensor was intended to monitor brain electrical activity. Another example is the electrocardiogram (ECG) sensor which was designed for monitoring heart activities[19]. WBAN collects real-time biomedical data such as changes in a patient's vital signs heart rate, blood pressure, and pulse They communicate with a special coordinator node, which is generally less energy-constrained and has more processing capacities. Then it is responsible for sending the data of the patient to a remote medical server through mobile devices such as a personal digital assistant (PDA) or a smartphone. Based on this data, doctors and other medical personnel could get a patient's status and allow them to take sensitive decisions or actions depending on the information acquired from those sensors [20].

WBAN common architecture consists of three tiers of communications: Intra-Body Area Networking (BAN) communications, Inter-BAN communications and beyond-BAN communications [21]. Intra-BAN communications see in Fig. 2 a) denote communications among wireless body sensors and the master node of the WBAN. Inter-BAN communications see in Fig. 2b) involve communications between the master node and personal devices such as notebooks, home service robots, and so on.

The beyond-BAN tier see in Fig. 2c) connects the personal device to the Internet. The data collected or transmitted in WBANs are very sensitive and must be protected against unauthorized access that could be dangerous to the life of the patient and sometimes lead to death [22]. Thus, scalable and strict security mechanisms are mandatory and should be handled, transmitted, and stored with care to prevent information leakage to unauthorized users. Therefore, authentication, data confidentiality, integrity, non repudiation, and privacy preservation should be guaranteed during all communications within the WBAN environment.

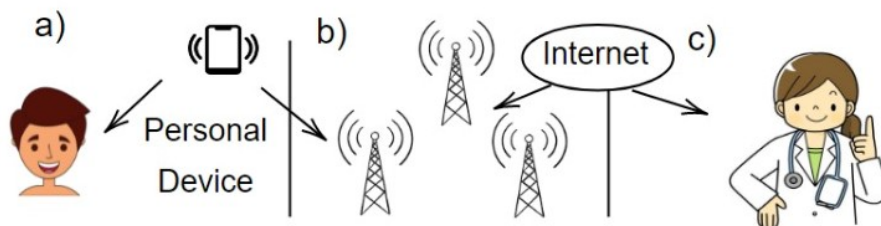


Figure 2: WBAN common architecture consists of three tiers of communications: a) Intra-BAN communications, b) Inter-BAN communications and c) beyond-BAN communications

3.2. Wireless Body Area Network technologies

3.2.1. IEEE 802.15.1 (Bluetooth)

Bluetooth technology is a short-range wireless communication standard, that can transport facts at speeds up to 3 Megabit per second (Mbps) over distances of up to 10 meters, thanks to this technology, each device can simultaneously communicate with

up to seven other devices, one device act as a master and up to seven others as slaves for the lifetime of the piconet [23] as shown in Fig. 3. Another key feature is the ability of devices to communicate without the need for line-of-sight positioning of connected devices. Thus, it is widely used for connecting a variety of personally carried devices to support data and voice applications. Bluetooth devices operate in the 2.4 GHz Industrial, Scientific and Medical band (ISM band), utilizing frequency hopping among 79 1 Megahertz (MHz) channels [24]. It can be used for sensors of relatively high data rate requirements. However, Bluetooth devices take a lot of power and time for continuous synchronization, therefore battery life may not endure for weeks. Automatic networking is not recommended since if a network’s owner leaves, the entire network will collapse.

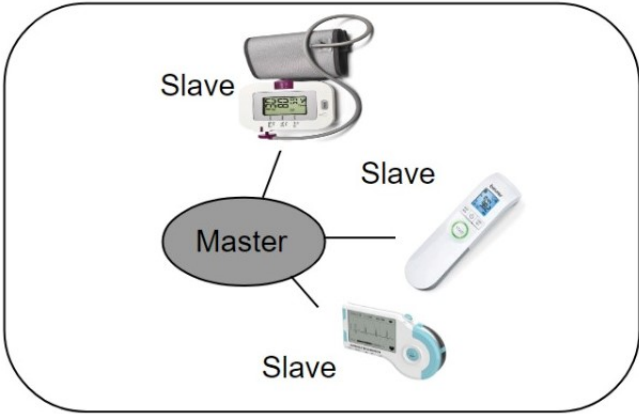


Figure 3: Bluetooth Architecture

A derived option of the Bluetooth standard is the Bluetooth Low Energy (BLE) 7, It was designed to wirelessly connect small devices to mobile terminals. which was introduced as a more suitable choice for WBAN applications where less power consumption thanks to the low duty cycle, BLE consumes 90% lesser than the power required by Bluetooth. his leads to extend the lifetime of the sensor’s battery in WBAN systems. Bluetooth Low Energy technology is expected to provide a data rate of up to 1 Mbps [21]. Using fewer channels for pairing devices, synchronization can be done in a few milliseconds compared to Bluetooths seconds.It uses 2.4 Gigahertz (GHz) frequency and the time needed for connection setup and data transfer is less than 3 milliseconds.Its

nominal data rate, low latency, and low energy consumption make BLE suitable for communication between the wearable sensor nodes and the access point. However, interference with other devices might be an issue as the technology operates in the 2.4GHz ISM band.

3.2.2. Ultra-Wideband-IEEE 802.15.3

Ultra-wideband (UWB) radio transmission is a high-rate, ultra-low control, short-go radio system innovation fit for moving information at a rapid by using more extensive transfer speed than the conventional "slender band" radio transmission advancements. That works over short distances and has excessive radio signal sensitivity. It has the ability to send data at extremely high speeds. This is achieved by delivering data across a far greater bandwidth than is typically available with traditional "narrowband" radio transmission systems. UWB technology provides various advantages for personal area networks (PANs) see in Fig. 4. Low power consumption (1mW/Mbps) and fast data rates are only a couple of the advantages of this technology (up to 480 Mbps). Because of these qualities, UWB is an excellent choice for WBAN applications that require a large amount of bandwidth but not a large amount of power [25] and [26]. The main physical section (which works in 2.4GHz ISM band) goes for a RF baseband and front-end processor improved for short-expand conveyance showing a present channel of under 100 mA which makes it small enough to be included in consumer devices.

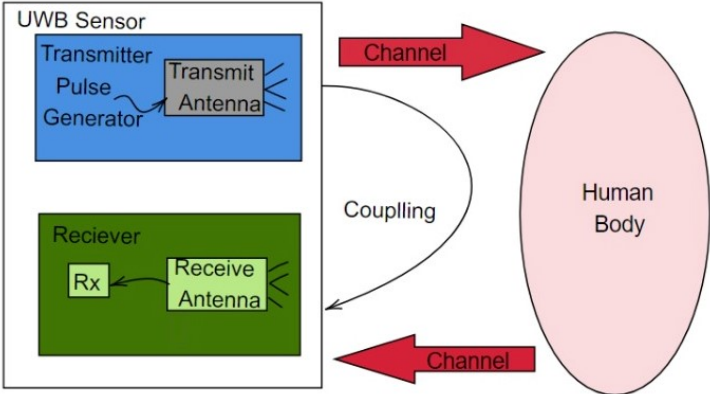


Figure 4: Block of scheme of the UWB medical scenario

3.2.3. ZigBee-IEEE 802.15.4

ZigBee is a short-distance wireless technology. It has the characteristics of low cost, low power consumption and low speed. Through the sleep mode, ZigBee enabled devices are capable of being operational for several years before their batteries need to be replaced . With a transmission range of ZigBee is 10 to 100 meters, ZigBee radio transmit data at speeds of 20 Kilobit per second (kbps), 40 kbps, and 250 kbps using this spectrum, which includes the frequencies 686 MHz, 915MHz, and 2.4GHz [27]. For WBAN,ZigBee targets medical applications that require frequent measurements and text-based data transmission with low power consumption such as body temperature monitoring, for the pulse monitoring and others. A significant disadvantage of ZigBee for WBAN applications is high levels of interference caused by the presence of IEEE 802.11b (WiFi), IEEE 802.15.1 (Bluetooth), and other wireless technologies in the same frequency range (band) which makes it difficult to implement it in hospitals for multiple patients [25]. In fact, due to the low data rate, it is difficult to implement in hospitals or clinics due to the quantity of multiple patients.

3.2.4. WiFi – IEEE 802.11

WiFi comes generally with four standards (802.11 a/b/g/n), it can operate in the 2.4 and 5 GHz bands and has a coverage of 100 m. It is able to deliver data rates of up to 600 Mbps. It is ideally suited for large data transfers by providing high-speed wireless connectivity and allowing video conferencing, voice calls and video streaming [21]. An important advantage is that all smartphones, tablets and laptops have WiFi integrated. WiFi is a high-power, high-speed wireless local-area network (WLAN) technology that can operate in the ISM band without a license. WiFi consumes five times the power of Bluetooth, WBAN sensor devices cannot last more than a week on a single charge. WiFi also has the disadvantages of breadth and complexity of protocol stack, which necessitates the use of additional resources like as memory and processing speed. A regular WBAN sensor node may not have this capability [28] and [23]. As Bluetooth and ZigBee, WiFi occupy the ISM bands, where serious co-channel interference may occur.

Table 1: Characteristics Wireless Body Area Network technologies

Propierties	IEEE 802.15.1 (Bluetooth)	Ultra- Wideband-IEEE 802.15.3	ZigBee-IEEE 802.15.4	WiFi – IEEE 802.11
Bad width	Up to 3 Mb/s	Up to 250 Kb/s	Up to 27.24 Mb/s	Up to 150 Mb/s
Power consup- tion	100mW	50 mW	Up to 250 Kb/s	800 mW
Comunication Range	Medium 100m	Low Up to 30m	Low Up to 75 m	High Up to 250m
Application	Low-bandwidth cable replace- ment	High-bandwidth cable replace- ment	Remote control, sensors	Internet Brows- ing, pc network- ing, file transfers

3.3. Applications of Wireless Body Area Network

WBAN medical applications and requirements WBAN supports many applications and has great practicality and advantages in daily life where it provides the advantages of freedom of movement, security, low power consumption, real-time data delivery and low cost [21]. WBAN Applications Wireless body area network applications are proving themselves very efficiently and these applications are not just for human health care monitoring but there are also many other applications such as sports, fitness, gaming, electronics, measuring body position, location of a person, military and many other that are using WBAN approach for different purposes. It takes the human body as the application carrier, turns it into a part of the communication network, truly realizes the ubiquitous network and omnipresent service, and playsan important role in the following areas [28].

Medical care services and chronic disease surveillanc see in Table 2 : These are the most important applications. There has been no good solution for the prevention and treatment of chronic diseases, worldwide [29]. The emergence of WBAN brings hope

for the treatment and prevention of various chronic diseases. Through the real-time comprehensive analysis and processing of the collected physiological information, we can effectively prevent and treat the disease, before and during onset. We can also save the physiological information of the disease for subsequent diagnosis, treatment, and medical research. The most important thing is that patients can get rid of the trouble of wired monitoring and experience the convenient service of remote medical monitoring [30].

Assistance for special groups, such as the disabled and the elderly: Sensor devices are worn on the limbs of blind people, which can perceive the surrounding environment and road information, in real-time, to provide navigation and position services for blind people. Developing a care system for the elderly which can sense the actions of the elderly and make corresponding reminders, by locating the elderly, and record the activities to provide security and safety of the elderly [31].

Covid-19: a case study In this section, we investigate the WBAN application for Covid-19 case study. Monitoring Covid-19 remotely may highly reduce the healthcare cost and increases the hospitals' capacity by decreasing the physical presence of the patients. By using biomedical sensors for health monitoring with the wireless technologies, it is possible to send medical reports to the medical staff where doctor's advice is obtained without the need of any physical movement [37]. This WBAN system comes as a rescuer for Covid patients who need to be under monitoring, especially for elderly patients and for patients suffering from chronic diseases. Hence, two scenarios are proposed for transmitting the patient's data to the medical server. In a first scenario, for the first tier it is possible to connect the sensors to the PD using BLE or ZigBee providing a data transmission for short distance which is convenient for the WBAN's first tier [21]. After been processed, the data must be sent to a gateway using WiFi or cellular networks. Finally, the data is received by the medical staff where the patient is diagnosed and an advice should be given in case of unstable condition. In another scenario, data is sent directly from the sensors to a gateway through one of the Low-power wide-area network (LPWAN) technologies providing a long range, low data rate and high network lifetime which are convenient for our case.

Table 2: Different WBAN application

Reference	Application	Contribution
[31]	It uses Bluetooth communication to measure body temperature, heartbeats, and possible falls	It implements power by solar energy
[32]	Assesses patient vibrations to determine whether the patient suffers from Parkinson's disease (PD).	The system makes it possible to determine the evolution of the disease.
[33]	It measures the kinematics of the patient's gait to determine if they have PD.	Implement sensors in the lower limbs and upper body.
[34]	Sensors placed on the soles of the feet to determine whether the patient suffers from PD.	Mobile application was implemented to monitor the patient.
[35]	Sensors in the lower body to determine whether the patient suffers from PD.	It uses ZigBee technology and protocols.
[36]	EEG sensor for assessing different brain activities	Uses ensemble classifier for epileptic seizure detection for imperfect EEG data

Other applications: WBAN applications are used to improve sports monitoring applications, the athletes physiological data collected during a game such as temperature, heart rate and body position may avoid critical situations [38] providing fire fighters with special environment monitoring (such as fire scene, toxic gas environment, etc.), warning firefighters regarding their own safety when their endurance threshold has exceeded; and, in the military, transferring important military intelligence to control centers or remote command troops, through wireless means. With the development of sensor technology and wireless network transmission technology, WBAN will be more and more widely used in medicine, including health monitoring, sports, entertainment, military, and aerospace fields, in the future [39] see in Fig 5. It also has considerable social value and economic benefits. Trouble of wired monitoring and experience the convenient service of remote medical monitoring

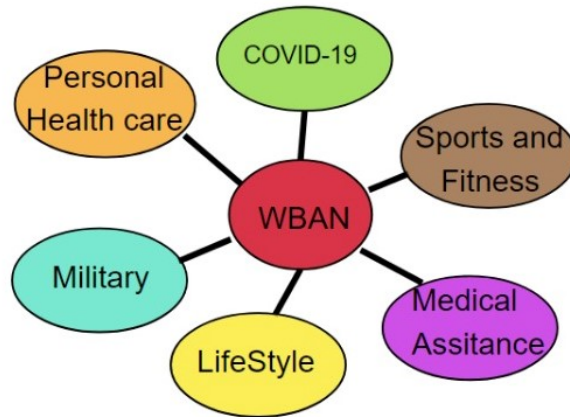


Figure 5: Applications of WBAN

3.4. Human Body Chanel

Communication techniques based Radio frequency (RF) or non-RF can be used for WBAN. non-RF technique uses human body as the communication channel. Such non-RF based technique is commonly known as human body communications (HBC) technique. HBC uses the human body as a signal transmission guide for electrical signals to interconnect devices in wireless body area networks (WBANs) [40]. Since body tissues show high conductivity, low-power signals can be transmitted at lower

frequencies without the need for using antennas, making consumption reduction possible. In addition, the signal is mainly confined to the human body surface, presenting little influence of electromagnetic noise and obstacles on transmission, and Intra Body Communications (IBC) helps to reduce wires of the wearable devices, thus contributing to reducing size and weight [41]. These advantages have led IBC to be included in the IEEE 802.15.6 standard as a third physical layer designated as human body communication (HBC) [42].

Whenever any form of energy is introduced into the human body, it is important to understand what risks might result from applying energy to internal tissue [43]. There are multiple standards defined on the exposure of the human body to electrical current such as the International Commission on Non-Ionizing Radiation Protection (ICNIRP) [44]. The Institute of Electrical and Electronics Engineers (IEEE) Standard and the National Institute for Occupational Safety and Health (NIOSH) Standards look into the effect of high voltage and current on the human body [45]. ICNIRP see in Table 3, considers that the lowest threshold across the cohort would have been approximately 100 mA for Occupational people it means All exposure to EMF experienced by individuals in the course of performing their work and 45 for general public [44].

Table 3: Reference levels for current induced in any limb, averaged over 6 min, at frequencies from 100 kHz to 110 MHz.

Exposure scenario	Frequency Range	Electric current, I (mA)
Occupational	100 kHz-110 MHz	100
General Public	100 kHz-110 MHz	45

3.5. Parameters and Electric Properties

3.5.1. Dielectric properties of a human body

The human body is not uniform, it consists of different types of tissues that have unique dielectric properties. There is a commonly used online database [46], which

provides the dielectric properties of body tissues at different frequencies. The database is based on results published in [47]. In Fig. 6 and Fig. 7 show relative permittivity (ϵ_r) and electrical conductivity (σ) in the frequency range of 30 kHz to 200 MHz. For a dry skin, conductivity is directly proportional to the frequency increases while the Relative permittivity is indirectly proportional to the frequency. When a signal is induced to the human body, via an electrode, an electric field is originated around the human body (assuming that there are proper connections to ground). The electric field strength at a distance R from a charge Q can be derived from Maxwell's equations[48] and[49]. and it is given as Ec.1

$$E = \frac{Q}{4\pi\xi R^2} = \frac{Q}{4\pi\epsilon_r\epsilon_0 R^2} \quad (\text{Ec.1})$$

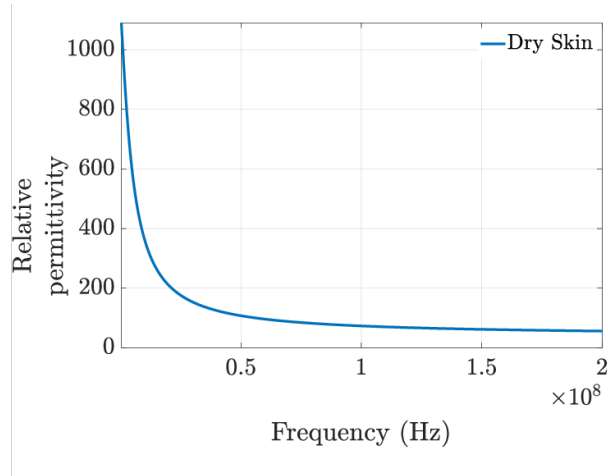


Figure 6: Measurements of the relative permittivity of Dry Skin by Gabriel and Gestblom [1]

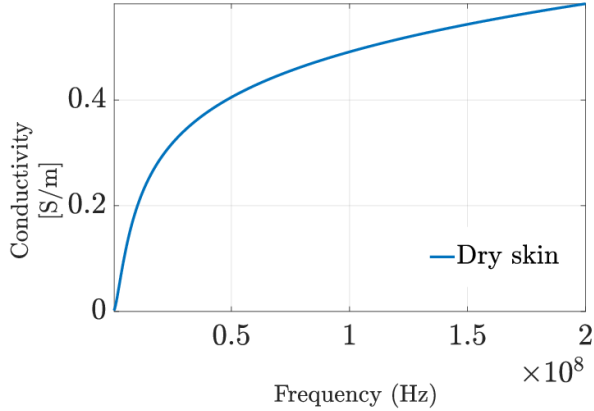


Figure 7: Measurement of the conductivity (S/m) of Dry Skin by Gabriel and Gestblom [1]

3.5.2. Path loss

Although in many HBC applications, an electrode is always connected to the skin or a conductive metallic plate touches the skin of a fingertip, we are interested on how tissues below the skin affect the electric field strength, and thus how much the communication performance is affected. The electric field penetrates the skin; thus, the tissue beneath the skin is expected to have an impact on the electric field strength.

Besides the quality of a HBC wireless link is affected by a variety of different factors: electrode material and size, operation frequency, coupling between the transceiver and the human body, distance between the transmitter and the receiver, size of the transmitter's and the receiver's ground planes, number of electrodes attached to a body, the body structure, body position, movement of a body, and impedance matching. Different electrode sizes are compared in [50]. It is noticed that the electrode resistance increases as the electrode size is decreased. The authors also report that there are significant differences between commercial electrodes even though they are made of same material (i.e., silver-silver chloride (Ag/AgCl)). The path loss changes significantly as a function of frequency. The path loss at 21 MHz, which is the center frequency of IEEE Std. 802.15.6 HBC PHY, is around 36 dB at 1.2 m distance [51]. In [52] the authors note that the environment does not impact the channel characteristics.

Achieve impedance matching and improving transmissions is one goal of HBC to accomplish this is important to analyze the input impedance, Z_{in} , between the excitation points, whose loads are the electrodes, phantoms model, and the space around the phantom [51]. There are three impedance related to electrodes 1) a signal-ground pair impedance; 2) each individual electrode impedance; and 3) an electrode-medium impedance. The impedance is dependent on the arrangement of the electrodes [53]. For capacitive electrodes, their show has a vertical structure, with signal and ground electrodes separated by a dielectric. This creates a capacitance between the electrodes that can be modeled as a common parallel plate capacitor, with $C_e = \epsilon L^2/d$, where ϵ is the permittivity of the material between the electrodes, L is the length of the electrodes, and d is the distance between them. For the electrode itself, the representation is dependent on the material and type of electrode [54] For a signal electrode in contact with the skin, the model is dependent on the type of electrode contact [54]. However, the channel gain does not change considerably for different electrode types as shown in [55], and [56], [52].

3.6. HBC Transmission Systems

3.6.1. Capacitive Coupling Body Transmission

Capacitive coupling (CC) was introduced by Zimmerman [57] in 1995 the signal electrodes both of TX and RX are exposed to the body, The GND electrodes of both TX and RX are floated in the air [58] shown in Fig. 8. In this way, the transmitter generates an electric potential, inducing an electric field in the body that is sensed by the receiver electrodes. The floating electrodes are coupled to ground through the air, creating a return path, while the signal electrodes in contact with the skin create the forward path of the signal. The existence of an external path means that capacitive coupling is only suitable for wearable devices and is critical because the return path is constituted through the environments [59].

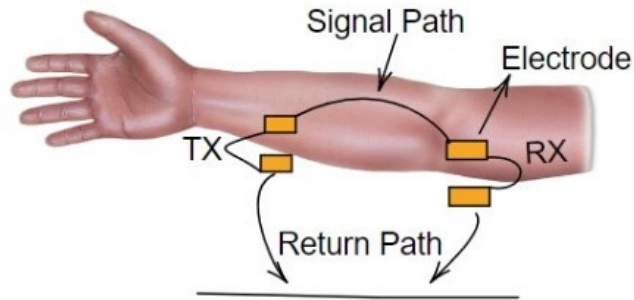


Figure 8: Capacitive Coupling HBC

3.6.2. Galvanic Coupling Body Transmission

Galvanic coupling was proposed by Wegmueller et al. [60] in which two electrodes of both TX and RX required direct contact between the electrode and skin.[61] shown in Fig. 9. Both the signal (forward) path and the return (backward) path are formed through the body, which is used as a transmission line. This method has a beauty of in susceptibility to the surrounding environment and It is mainly characterized by the dielectric properties of tissues between the transceivers [59]

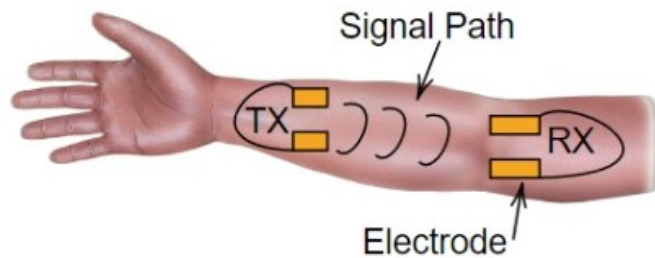


Figure 9: Galvanic Coupling HBC

3.7. Two-Port Network Theory

Two-port network theory is a circuit analysis technique that is different from the majority of other approaches. Most circuit analysis approaches (Kirchhoff’s laws, node voltage/mesh current methods, superposition, and others) provide a way of calculating voltages and currents anywhere in the circuit. Thevenin or Norton theorems allow us to obtain an equivalent circuit model with respect to the specified pair of terminals (usually the output terminals, or the output port) of the network [62].

Another way of describing the circuit with respect to the two terminals is by treating the network as a two-port circuit. In many electrical circuits obtaining voltages and currents at the input and output ports, instead of any point in the circuit, is more convenient and practical. Thus, the fundamental principle underlying the two-port circuit analysis is that only the terminal variables (input voltage/current and output voltage/current) are of interest. We are not interested in calculating voltages and current inside the circuit [63].

In Electromagnetic compatibility (EMC) the two-port network analysis is usually carried in a sinusoidal steady-state where the voltages and currents are sinusoids and as such, at each frequency, are described by their amplitudes and phases [63]. It turns out that such an analysis can be easily performed using complex numbers, called phasors, (instead of real time functions) which represent these amplitudes and phases. To differentiate a complex variable from a real variable let’s place a “hat” above it. Thus, V and I denote real variables, while \hat{V} and \hat{I} correspond to the complex ones. Figure 1 shows the basic building block of a two-port network.

3.7.1. Scattering Parameters

Scattering refers to the way in which the traveling currents and voltages in a transmission line are affected when they meet a discontinuity caused by the insertion of a network into the transmission line [48]. S-parameters can be saved e.g. as a S4P-file that contains all the combinations of the reflection and transmissions in a network, and this shows how the device under test behaves with a signal in both forward and reverse

directions.

In RF design, we can't use other parameters for analysis such as Z, Y, H parameters as we can't do short circuit and open circuit analysis as it is not feasible. For a two port network show in Fig.10. s-parameters can be defined as

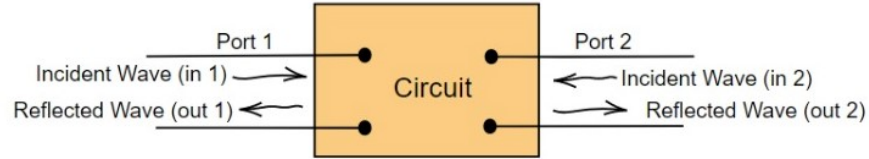


Figure 10: Two port network

S_{11} is the input port voltage reflection coefficient see in [Ec.2](#)

S_{12} is the reverse voltage gain see in [Ec.3](#)

S_{21} is the forward voltage gain see in [Ec.4](#)

S_{22} is the output port voltage reflection coefficient see in [Ec.5](#)

$$S_{11} = \frac{out_1}{in_1} \quad (Ec.2)$$

$$S_{12} = \frac{out_1}{in_2} \quad (Ec.3)$$

$$S_{21} = \frac{out_2}{in_1} \quad (Ec.4)$$

$$S_{22} = \frac{out_2}{in_2} \quad (Ec.5)$$

The S-parameter matrix can be used to determine reflection coefficients and transmission gains from both sides of a two port network. This concept can further be used to determine s-parameters of a multi port network. These concepts can further be used

in determining Return loss. It can be thought of as a measure of how close the actual input/output impedance of the network is to the nominal system impedance value.

3.7.2. Z Parameters

Z parameters (also known as impedance parameters or open-circuit parameters) are properties used in electrical engineering to describe the electrical behavior of linear electrical networks. These Z-parameters are used in Z-matrixes (impedance matrixes) to calculate the incoming and outgoing voltages and currents of a network see in: [Ec.8](#), [Ec.9](#), [Ec.10](#) and [Ec.11](#).

Z-parameters are also known as “open-circuit impedance parameters”, as they are calculated under open-circuit conditions see in [Ec.6](#). That is to say that $I_x=0$, where $x=1, 2$ refers to the input and output currents flowing through the ports of a two port network. The Z-parameter matrix for the two-port network is probably the most common. In this case the relationship between the port currents is see in [Ec.7](#) This is why these parameters are called either impedance parameter or Z parameter.

$$I_1 = 0, I_2 = 0 \tag{Ec.6}$$

The values of these Z parameters of a two port network, can be evaluated by making once

$$\begin{pmatrix} V_1 \\ V_2 \end{pmatrix} = \begin{pmatrix} Z_{11} & Z_{12} \\ Z_{21} & Z_{22} \end{pmatrix} \begin{pmatrix} I_1 \\ I_2 \end{pmatrix} \tag{Ec.7}$$

Where:

$$Z_{11} = \frac{V_1}{I_1} \tag{Ec.8}$$

$$Z_{12} = \frac{V_1}{I_2} \tag{Ec.9}$$

$$Z_{21} = \frac{V_2}{I_1} \quad (\text{Ec.10})$$

$$Z_{22} = \frac{V_2}{I_2} \quad (\text{Ec.11})$$

3.7.3. Transmission Lines: Reflection Coefficient, VSWR and Power Transmitted

We are now aware of the characteristic impedance of a transmission line, and that the tx line gives rise to forward and backward travelling voltage and current waves. We will use this information to determine the voltage reflection coefficient, which relates the amplitude of the forward travelling wave to the amplitude of the backward travelling wave.

To begin, consider the transmission line with characteristic impedance see in Fig 11 Z_0 attached to a load with impedance Z_L :

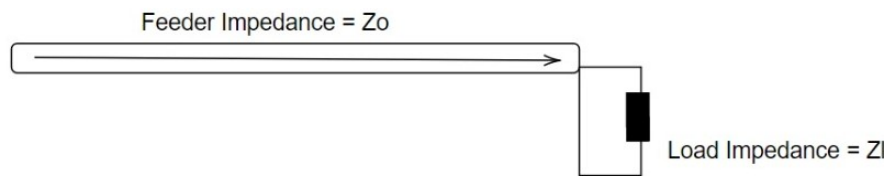


Figure 11: reflection

At the terminals where the transmission line is connected to the load, the overall voltage must be given by see in Ec.12:

$$Z_l = \frac{V}{L} \quad (\text{Ec.12})$$

The ratio of the reflected voltage amplitude to that of the forward voltage amplitude is the voltage reflection coefficient. This can be solved for via the above [Ec.13](#):

$$r = \frac{V^-}{V^+} = \frac{Z_l - Z_0}{Z_l + Z_0} \quad (\text{Ec.13})$$

The reflection coefficient is usually denoted by the symbol gamma. Note that the magnitude of the reflection coefficient does not depend on the length of the line, only the load impedance and the impedance of the transmission line. Also, note that if $Z_L=Z_0$, then the line is "matched". In this case, there is no mismatch loss and all power is transferred to the load. At this point, you should begin to understand the importance of impedance matching: grossly mismatched impedances will lead to most of the power reflected away from the load.

SWR

SWR is sometimes called VSWR, for voltage standing wave ratio, is defined as the ratio between transmitted and reflected voltage standing waves in a radio frequency (RF) electrical transmission system. It is a measure of how efficiently RF power is transmitted from the power source, through a transmission line, and into the load. A common example is a power amplifier connected to an antenna through a transmission line.

SWR is, thus, the ratio between transmitted and reflected waves. A high SWR indicates poor transmission-line efficiency and reflected energy, which can damage the transmitter and decrease transmitter efficiency. Since SWR commonly refers to the voltage ratio, it is usually known as voltage standing wave ratio (VSWR).

In the typical ham station setup, a transmitter is connected to a feed line, which is then connected to the antenna. When you key the transmitter, it develops a radio frequency (RF) voltage on the transmission line input. The voltage travels down the feed line to the antenna at the other end and is called the forward wave. In some cases, part of the voltage is reflected at the antenna and propagates back down the line in the reverse direction toward the transmitter, much like a voice echoing off a distant cliff. SWR is a measure of what is happening to the forward and reverse voltage waveforms

and how they compare in size.

Standing wave ratio (SWR) is defined as the ratio of the maximum magnitude of the standing wave to minimum magnitude of the standing wave. In terms of the potential [Ec.14](#) and [Ec.15](#):

$$SWR = \frac{\textit{maximum}}{\textit{minimum}} \quad (\text{Ec.14})$$

Therefore:

$$SWR = \frac{1 + r}{1 - r} \quad (\text{Ec.15})$$

Note that SWR ranges from 1 for perfectly-matched terminations ($r = 0$) to infinity for open- and short-circuit terminations ($r = 1$). It is sometimes of interest to find the magnitude of the reflection coefficient given SWR [Ec.16](#).

Solving Equation

$$r = \frac{SWR - 1}{SWR + 1} \quad (\text{Ec.16})$$

SWR is often referred to as the voltage standing wave ratio (VSWR), although repeating the analysis above for the current reveals that the current SWR is equal to potential SWR, so the term “SWR” suffices. $SWR < 2$ or so is usually considered a “good match,” although some applications require $SWR < 1.1$ or better, and other applications are tolerant to SWR of 3 or greater.

Power Reflected

Issues arise when power is transferred into the transmission line or feeder and it travels towards the load. If there is a mismatch, i.e. the load impedance does not match that of the transmission line, then it is not possible for all the power to be transferred. As power cannot disappear, the power that is not transferred into the load has to go somewhere and there it travels back along the transmission line back towards the

source see in Fig 12:.

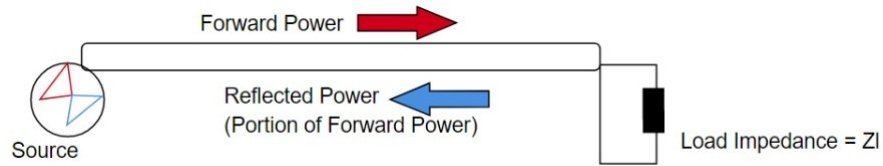


Figure 12: Reflection

When this happens the voltages and currents of the forward and reflected waves in the feeder add or subtract at different points along the feeder according to the phases. In this way standing waves are set up.

Using the Sparameters we have [Ec.17](#):

$$RL = -10\log\frac{P_{ref}}{P_{inc}} \quad (\text{Ec.17})$$

And its relationship with SWR is shown in the following table. Table 4 shows the Percentage of Reflected Power vs SWR

Table 4: Measurements of electrodes with VNA in diferents mediums

VSWR	% Power Reflected
1:1	0
1.5:1	4
2:1	11
2.5:1	18
3:1	25
4:1	36
5:1	44
6:1	51
10:1	67

4. Materials and Methodology

In this work, we fabricated three pairs of different electrodes; three of them are for Capacitive Coupling (CC) and one for Galvanic Coupling (GC). For the CC ones, we fabricated two different shapes (circular and square) and two different excitation orientation (vertical and horizontal) studied their performance. In addition, we test one pair of electrodes on three different media: saltwater, gel, and human skin to study the impact of the electrodes on media.

In the following subsections, we discuss the electrode fabrication, mediums fabrication and the experimental setup, results, discussions. Finally, conclusions and future perspectives.

4.1. Equipment and Calibration

The transmission properties were investigated over a wide range of frequencies up to 30 kHz by measuring the channel response concerning three distances (4, 10 and 15) between Tx and Rx Fig. 13 shows two types of measurement setups are used for comparison. The first one is with a Mini Vector Network Analyzer (VNA) Pro and the

second one is with N9914B RF Fieldfox.

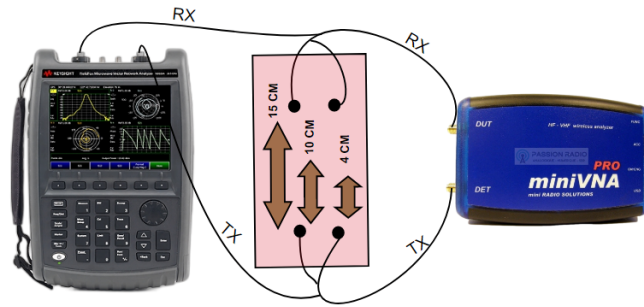


Figure 13: Setup to measure by using a VNA

As a first step a Mini VNA driver test and calibration must be done. The acronym SOLT standards for: Short, Open, Load, Through. It is one of the the most straightforward ways of calibrating an RF vector network analyzer. To undertake this form of VNA network analyzer user calibration known standards with a short circuit, open circuit, a precision load (usually 50 ohms) and a through connection are needed.

1. Select the menu ANALYZER and then SETUP
2. Choose right driver and COM port
3. Press the buttons Test (1) Update (2).
4. Select as Mode in the right bottom corner of the window “REFLEXION”
5. Select the menu CALIBRATION and then CREATE
6. Calibration in a sequential order As calibration frequency range from 100 kHz to 200 MHz is sufficient.
 - a) OPEN
 - b) SHORT
 - c) LOAD
7. Press “save” calibration press the “update” button (closes the window) see in Fig. 14

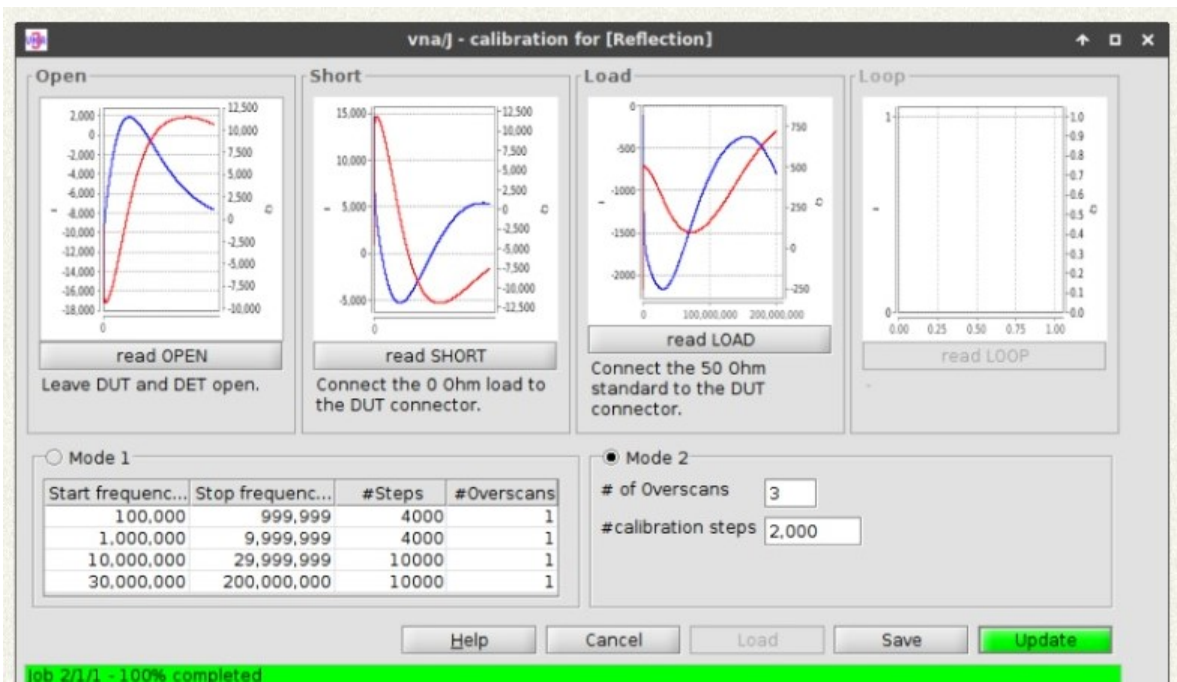


Figure 14: mini vna calibration pro using SOLT

As a second step was the calibration of N9914B RF Fieldfox. We use the same SOLT calibration see in Fig. 16, 15 and 17



Figure 15: Calibration Kit SOLT



Figure 16: Calibration in progress

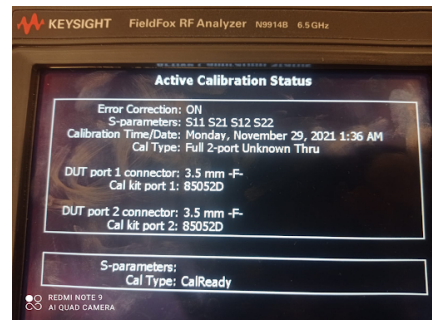


Figure 17: Calibration done for 4 S-Parameters

Besides, a LAN connection between the Handle Fieldfox and a laptop was made. Through the Software Keysight Connection Expert 2022, then we use the Software created on Labview. This Software allow us visualize, named and save the data directly

in our laptop. The software has a first sub vi is to add some configuration parameters such as Frequency Range, Number of sweep points, name of the researcher, calibration file see in Fig. 18. The second sub vi is used to obtain the 4-S parameters in on single file and saved them in a specific path see in Fig. 19. Besides, we can visualize in four graphs the data obtained see in see in Fig. 20.

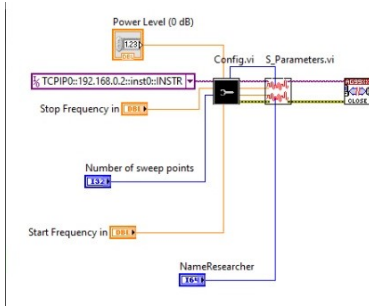


Figure 18: Software created in Labview

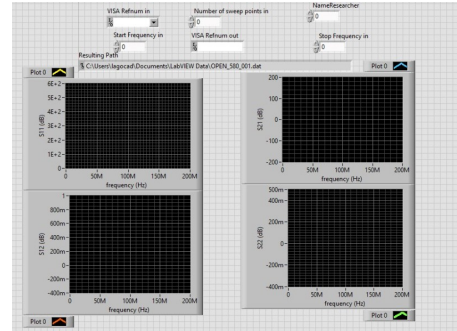


Figure 19: General View



Figure 20: Test

4.2. Phantom building

4.2.1. Salty water medium

Liquid phantoms were usually adopted in HBC trial due to they are easiest to prepare. In [56] the authors used an insulator (polyvinyl chloride bag) containing conductive liquid (salt water) to model the human arm as a cylinder. In [5], the authors used a liquid phantom filled in a plastic container 0.45% of NaCl and 2 gallons of water to characterized the body as transmission medium. Our medium, salt-water samples were prepared with 250, 600 and 1000 ml of Deionized water (DI) and different weight of sodium chloride to keep the concentration of salt (0.5 M) in each experiment, see Table 5 and Fig 21. Besides the transmitter (Tx) and receiver (Rx) are fixed to a

sponge to improve the stability of electrodes over the medium.

Sample No.	DI Water (ml)	Sodium Chloride (g)
1	250	29.2
2	600	70.1
3	1000	116.9

Table 5: Composition of Salty Water Samples.

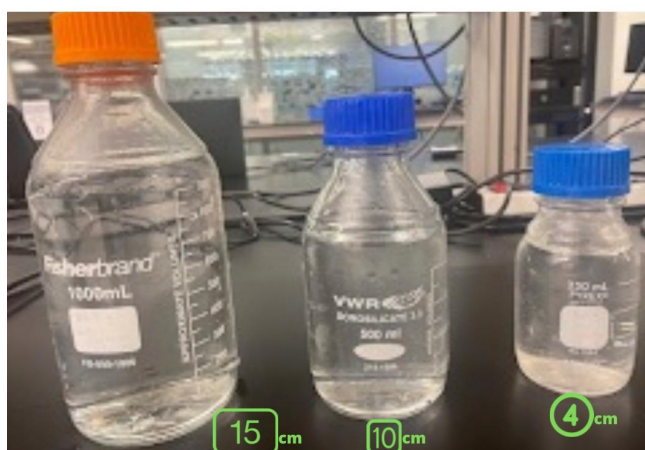


Figure 21: liquid samples

4.2.2. Gelatin Medium

All gelatins were prepared by dissolving its powder in deionized water at 80 °C. Gelatins with 10 % of concentration were prepared , as well 1 % of salt concentration was added [64].All gelatins solidified at room temperature, and then were placed in the refrigerator. The gelatins were removed from the refrigerator at least 24 hours prior to measurements, insuring these were carried out at room temperature. See in Table 6 and Fig 22.

Table 6: Gelatin Fabrication

Sample No.	DI Water (ml)	Gelatin (g)	Sodium Chloride (g)
1	250	25	2.5
2	600	60	6
3	1000	100	10

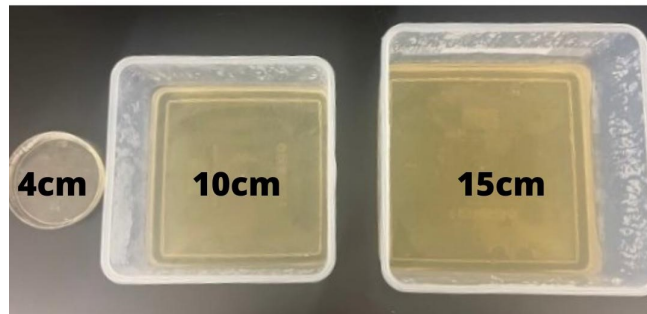


Figure 22: Gelatin samples

4.2.3. Human Arm

For measurement human body transmissions. One volunteer remained seated and two pairs of circular capacitive electrodes were attached. The RX electrode was attached on the forearm and TX was attached on the wrist. the electrodes were fixed by a wristband show in Fig 23. The distance between TX electrode and RX electrode was 4, 10 and 15 cm. Furthermore, the transmitter was connected to the Port 1 of pro mini vector network analyzer and the receiver was attached and connected to the Port 2 of VNA. Finally, the electrodes were evaluated in a frequency range from 100 KHz to 200Mhz using 1mW of transmitter power.



Figure 23: Experimental setup for Capacitive and Galvanic Coupling on a human arm, showing the current paths on human's body.

4.3. Electrodes Fabrication

The design of each proposed electrode is based on the FR4 epoxy substrate with dielectric constant 4.4. Half of the FR4 plates were used as insulator material so the copper of FR4 plates was removed as show Fig. 24 and we use a coaxial cable RG 59. Then, we use one extreme on the coaxial cable has a SMA connector which will be linked to the VNA devices and the other extreme is attached directly to the electrodes. The ground path comes from a the outer conductor of coaxial cable and the Signal path comes from the inner conductor. Fig. 25 shows a pair of Square Electrodes in a capacitive configuration, with a dimension of 20 mm x 20 mm x 1.6 mm. Fig. 26 shows Circular electrodes with a diameter of 2.5 cm. Fig. 27 shows Capacitive electrodes, coaxial cable is linked to circular electrodes horizontally, electrodes have a diameter of 2cm and 2.5 cm as Rx and Tx respectively. Fig. 28 shows Galvanic Electrodes two circular copper PCB of 2cm of diameter are used with a coaxial linked to the electrodes horizontally.

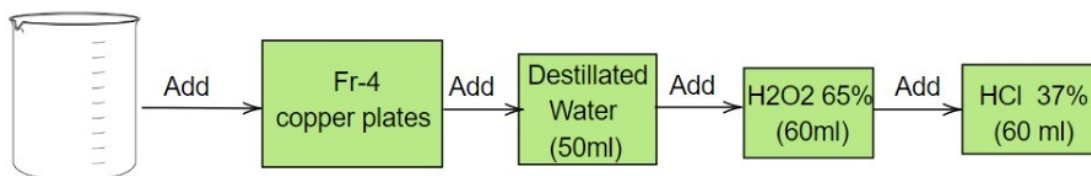


Figure 24: Insulator Material

4.3.1. Square electrodes

One extreme of coaxial cables is connected to SMA connector the other extreme of coaxial cable is connected to the electrodes. The square electrodes are capacitive, three plates of FR4 of 20 mm x 20 mm x 1.6 mm are used. The ground path comes from a coaxial cable RG (x) and is linked directly to the copper part of one plate of FR4. Then the signal path is linked to also the copper of the second Fr4 plate and the insulator plate is in the middle are shown in Fig. 25.



Figure 25: Square electrodes 2x2 cm

4.3.2. Circular electrodes

An extreme of coaxial cables is connected to SMA connector the other extreme of coaxial cable is connected to the electrodes. The outer conductor of coaxial cable was soldered on a circular copper part of 2.5 cm of a diameter of FR-4 plate then two circular FR4 plates without copper were used as insulator and the inner conductor of coaxial cable was solder to circular copper part of Fr 4 which could be attached to phantom directly is shown in Fig. 26.



Figure 26: Circular electrodes 2x2 cm

4.3.3. Planar Capacitive Electrodes

In this configuration of electrodes, the coaxial cable is linked to the electrodes horizontally and two circular FR4 plates of 2cm and 2.5 cm of diameters are used as Rx and Tx respectively. An extreme of coaxial cables is connected to SMA connector the other extreme of coaxial cable is connected to the electrodes. The ground path comes from a coaxial cable (Outer conductor) and is linked directly to the copper part of one FR4 plate. Then the signal path that comes from the inner conductor of the coaxial cable is linked to also the copper of the second FR4 plate which could be attached to the phantom directly. The part of FR-4 without copper is used as an insulator and there are put face to face as shown in Fig. 27.



Figure 27: Planar Capacitive electrodes 2.5 cm of diameter.

4.3.4. Planar Galvanic Electrodes

In this configuration of electrodes, the coaxial cable is linked to the electrodes horizontally and two circular Fr4 plates of 2cm in diameter are used. An extreme of coaxial cables is connected to SMA connector the other extreme of coaxial cable is connected to the electrodes. The outer conductor of coaxial cable was soldered on a circular copper part of FR-4 plate then the inner conductor of coaxial cable was solder to circular copper part of Fr 4 Both electrodes could be attached to phantom directly are shown in Fig. 28.



Figure 28: Planar Galvanic electrodes 2.5 cm of diameter.

4.4. ANALYSIS

We are now aware of the characteristic impedance of a transmission line, and that the tx line gives rise to forward and backward travelling voltage and current waves. We will use this information to determine the voltage reflection coefficient, which relates the the amplitude of the forward traveling wave with the amplitude of the backward traveling wave.

4.4.1. SWR

When using the mini VNA equipment, a csv file is obtained with the following information see in Table 7, we use the data obtained to calculate the reflection coefficient.

To find the SWR we use the data below to Magnitude and [Ec.18](#).

Table 7: Measurements of electrodes with VNA in diferents mediums

Frequency (Hz)	Returnloss (dB)	Returnphase (°)	Magnitude (r)
----------------	-----------------	-----------------	---------------

$$SWR = \frac{1 + r}{1 - r} \quad (\text{Ec.18})$$

4.4.2. POWER TRANSMITTED

From the values obtained in the return loss column, and with the next equations [Ec.19](#),[Ec.20](#),[Ec.21](#) and [Ec.22](#). We can obtain the percentage reflected in each experiment.

As Power Initial or Incident we use 1mW.

$$RL = -10 \log \frac{Power_{reflected}}{Power_{incident}} \quad (\text{Ec.19})$$

$$P_{ref} = \frac{P_{inc}}{10^{\frac{RL}{10}}} \quad (\text{Ec.20})$$

$$P_{ref} = \frac{1}{10^{\frac{RL}{-10}}} \quad (\text{Ec.21})$$

$$P_{ref}(\text{porcentaje}) = P_{ref} \times 100 \quad (\text{Ec.22})$$

Finally, we plot the percentage transmitted throughout our frequency band using the following equation [Ec.23](#).

$$P_{transmitted}(\text{porcentaje}) = 100 - P_{ref}(\text{porcentaje}) \quad (\text{Ec.23})$$

5. Results and Discussions

5.1. Results of Transmission data using different configuration of electrodes

Two different shapes of electrodes were investigated: circular and square, two different location of electrodes were used: vertical electrodes and planar electrodes. Finally capacitive and galvanic system were study under the following conditions: 1mW and frequency range from 100kHz to 100Mhz with a distance between the geometric centers of 4, 10, and 15cm in salt with water, ten consecutive times and averaged. Fig 29 shows the experimental trial using circular capacitive electroddodes in a salty liquid medium at 15 cm.



Figure 29: Experimental characterization of planar capacitive electrode at 15 cm

5.1.1. Results of Square Electrodes

Fig. 30a, shows return loss (S_{11}), represents how much power is reflected from the Tx Square electrodes at different distances When the electrodes are not in contact with the media (i.e., left floating in the air) all signal power is reflected from the electrodes. That means that all the power has been reflected and none has been transmitted. Besides in a salt water medium a higher loss (-12 dB) is acquired at 4 cm around 100MHz and in the rest of the experiment there is not a big loss. Fig. 30b, shows how much is the

signal delay in time. For frequencies, less than 27Mhz show a positive phase it means the output signal is leading the input, while the frequency increases it turns a negative phase resulting in a lagging (delayed) output signal

Fig. 30c, shows magnitude impedance. It suffers peaks of increasing, the higher peak is around 500 ohms at a distance of 10 cm the impedance keeps constant with a frequency higher than 100Mhz. Besides at a distance of 10 cm, the electrodes present higher impedance than 4 and 15 cm which could be possible due to contact between the sponge and the electrode in the sample. and how is supposed the input impedance of electrodes without the presence of conductive phantom (air) starts with an impedance to (infinity) and decreases with frequency increases. Fig. 30d shows a Nyquist plot acquired from Square electrodes, at lower frequencies it has inductive effects but since 27 MHz there are capacitive effects.

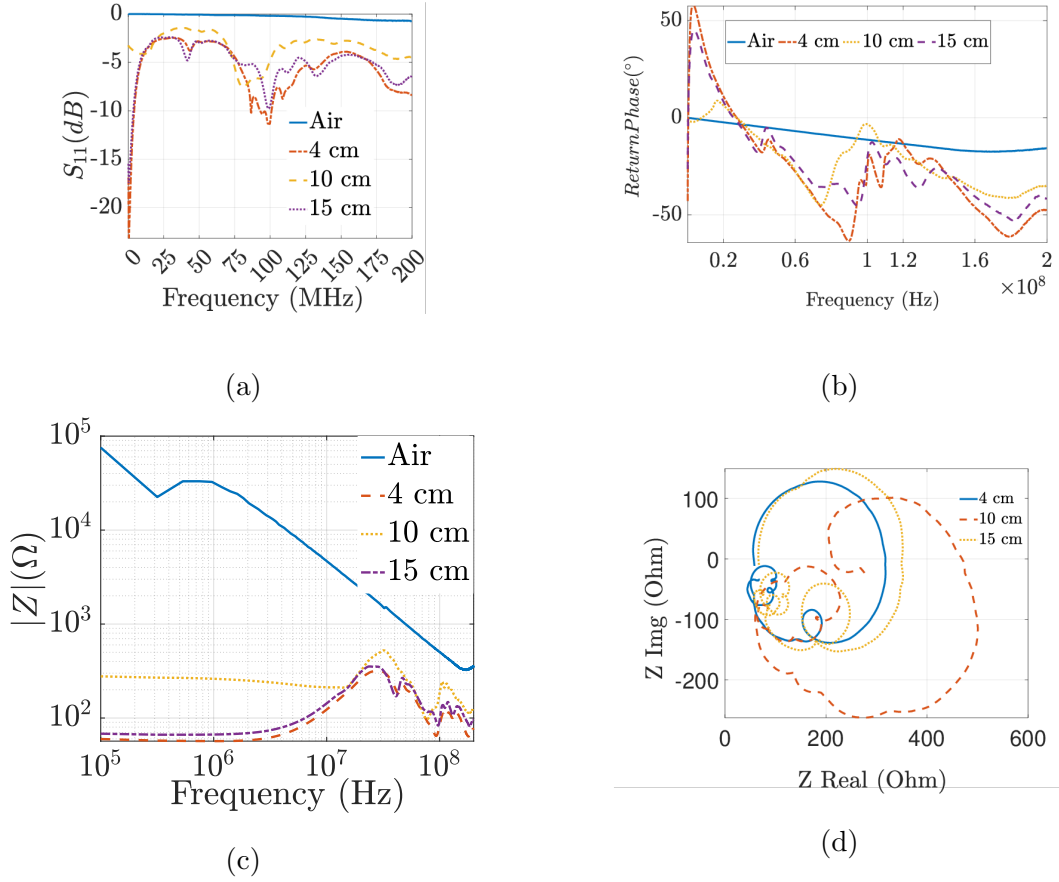


Figure 30: Capacitive Square axial electrodes. Return Loss (S_{11}) (a), Return Phase (b), Impedance modulus $|Z|$ (c) and Nyquist Plot (d)

5.1.2. Results of Circle electrodes

Mini Vector Network Analyzer Pro is exploited to measure S parameters, Magnitude of Impedance, and Phase using Circle electrodes in a saltwater sample with a distance between the geometric centers of 4, 10, and 15cm. All of them were evaluated from 100 kHz to 200 MHz, ten consecutive times and averaged. Fig. 31a, shows Return loss acquired from Circular electrodes at different distances, Firstly, there is no signal transmission by the air therefore S_{11} values are almost zero in the all frequency interval.

Conversely, the circular capacitive axial electrodes present a better performance. The values of S_{11} are almost -20 dB at 4 cm, -15 dB at 10 cm, and -10 dB for 15 cm. As the previous pair of electrodes, there are some peaks of better performance at frequencies of around 100 MHz (Fig. 31a). We can conclude that the use of square electrodes

should be discarded if working at high frequency.

Fig. 31b shows how much is the signal delay in time. For frequencies, less than 20 Mhz show a positive phase which means the output signal is leading the input, while the frequency increases it turns a negative phase resulting in a lagging (delayed) output signal. Except for the air medium which indicates that there is no transmission. Fig. 31c, shows magnitude impedance. The graph shows little peaks of increasing between 100KHz to 200Mhz. At 15 cm the higher peak is around 1000 ohms then the impedance keeps constant in a frequency higher than 100Mhz. During all the experiments the impedance increase when the distance between electrodes increases and impedance decrease with frequency increase until 300-400 Ohm and how is supposed the input impedance of electrodes without the presence of conductive phantom (air) starts with an impedance to (infinity) and decreases with frequency increases. Fig. 31d shows a Nyquist plot acquired from Square electrodes, at lower frequencies it has inductive effects from 25 MHz there are capacitive effects.

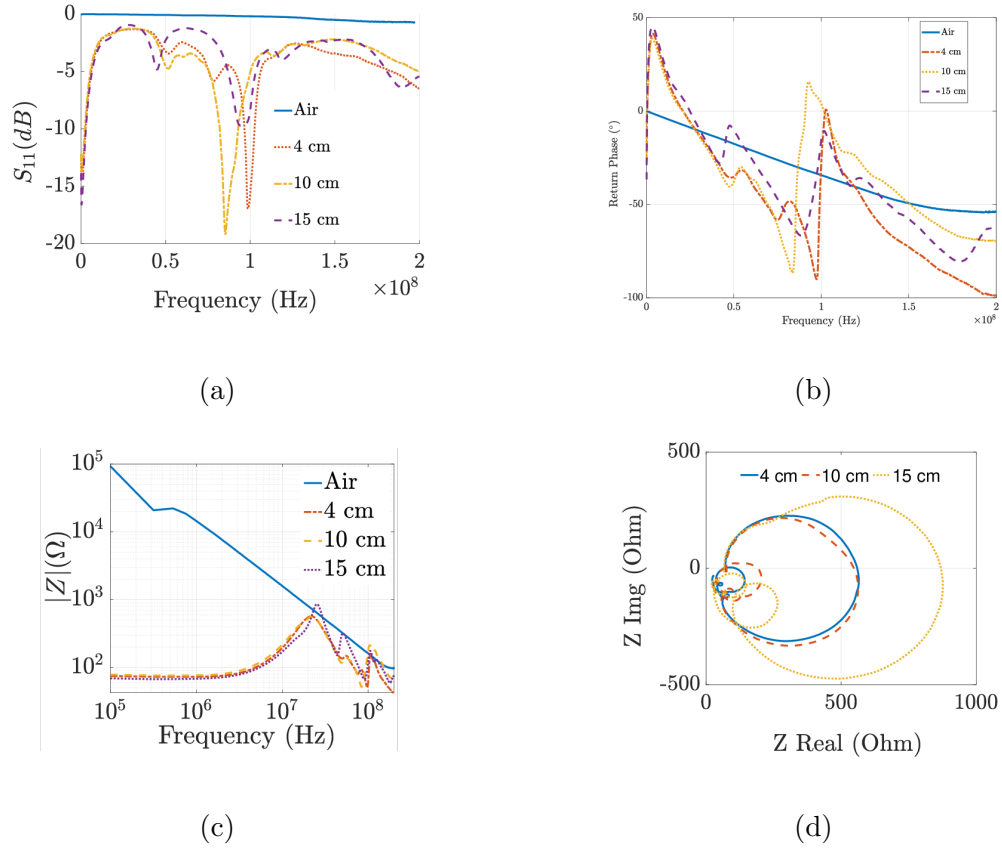


Figure 31: Circular Axis Electrodes electrodes for different separations. Return Loss (S_{11}) (a), Return Phase (b), Impedance modulus $|Z|$ (c) and Nyquist Plot (d)

5.1.3. Results of Planar Capacitive Electrodes

N9914B FieldFox Handheld RF Analyzer, 6.5 GHz is exploited to S parameters, Magnitude of Impedance, and Phase using Planar Capacitive electrodes. All of them were evaluated from 100 kHz to 200 MHz, which is the most important frequency band for HBC.

Fig. 32a, shows Return loss acquired from Capacitive electrodes at different distances, Rx has a diameter of 2cm and Tx has a diameter of 2.5cm. Firstly, Since the air path has the same insertion loss -5 dB compared to the body path in the 4 and 10 cm channel length, it is not included in the next step of our study. Then, at 4,10, and 15 cm there is a higher loss of transmission more than -15 dB is acquired in a frequency of 20MHz. Fig. 32b, shows how much is the signal delay in time. There is a constant

change between leading the input and a lagging (delayed) output signal even in the air medium which indicates that there is no transmission.

Fig. 32c shows magnitude impedance. The graph shows a tendency of increasing impedance when frequency increases. At 4 cm show a higher impedance around 100 ohms. At 15 cm presents less impedance than at 4cm until 100Mhz and how is supposed the input impedance of electrodes without the presence of conductive phantom (air) starts with an impedance to (infinity) and decreases with frequency increases. Fig. 32d shows a Nyquist plot acquired from Square electrodes, at air medium has an inductive behavior from all intervals of frequency and at 4,10 and 15 cm from lower frequencies it has inductive effects from 25 MHz there are capacitive effects.

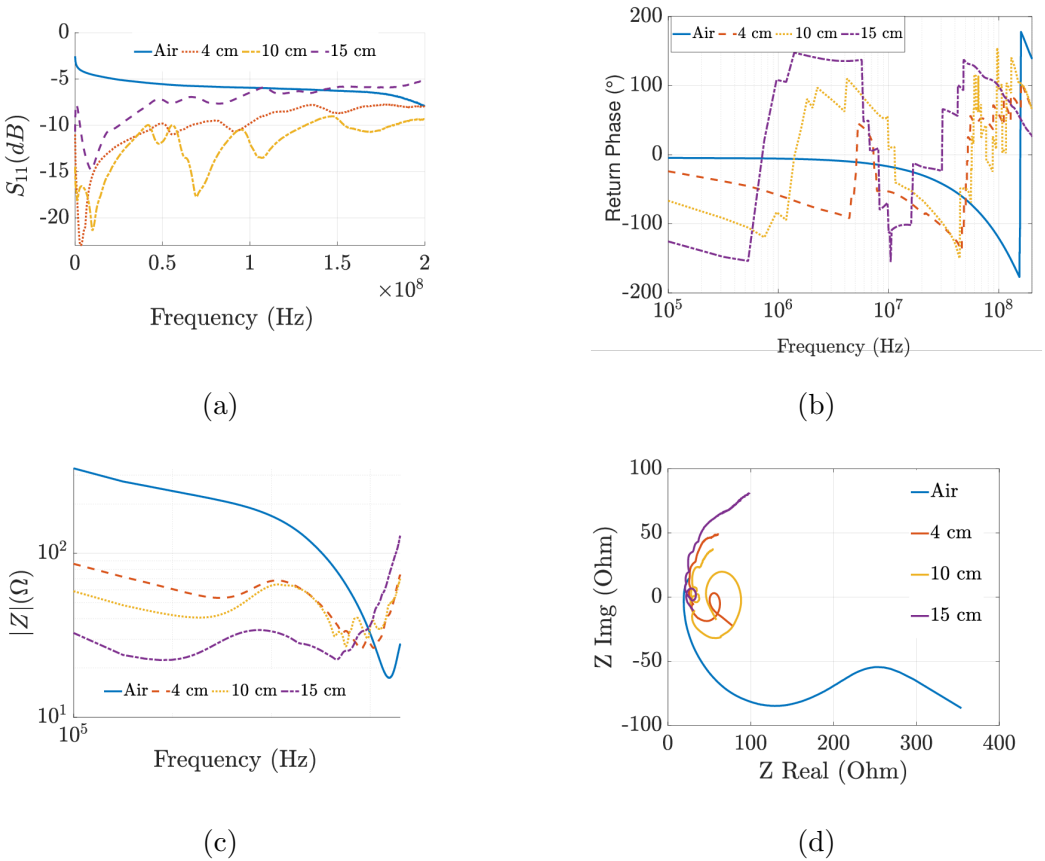


Figure 32: Planar Capacitive electrodes for different separations. Return Loss (S_{11}) (a), Return Phase (b), Impedance modulus $|Z|$ (c) and Nyquist Plot (d)

5.1.4. Results of Planar Galvanic Electrodes

N9914B FieldFox Handheld RF Analyzer, 6.5 GHz is exploited to S parameters, Magnitude of Impedance, and Phase using Planar Galvanic electrodes. All of them were evaluated from 30 kHz to 200 MHz, which is the most important frequency band for HBC. Fig. 33a, shows the average of all the reflection losses from 100 kHz to 200 MHz when the distance between TX and RX is 4cm, 10cm, and 15cm. The horizontal axis represents the frequency in kHz and the vertical axis represents the received signal power in dB. GC electrodes show overall S_{11} less than -6 dB which is needed to have good matching. The galvanic electrodes performance is better than the square and circular capacitive electrodes in the range 1–25 MHz, but for higher frequencies its return losses are more discrete, becoming apparently constant giving a value of -5 dB (Fig. 33a).

Fig. 33b, shows how much is the signal delay in time. For frequencies, less than 50 Mhz show a negative phase resulting in a lagging (delayed) output signal. After 50 Mhz there is a positive phase which means the output signal is leading the input. Fig. 33c, shows a higher impedance of those electrodes without conductive medium however $|Z|$ underwater samples show an impedance from 10 to 100 Ohms. Fig. 33d, shows a Nyquist plot acquired from Planar Galvanic electrodes, at 4 cm has capacitive behavior but from 24 MHz the electrodes present inductive effects. However at 10 and 15 cm has an inductive behavior from all interval of frequency.

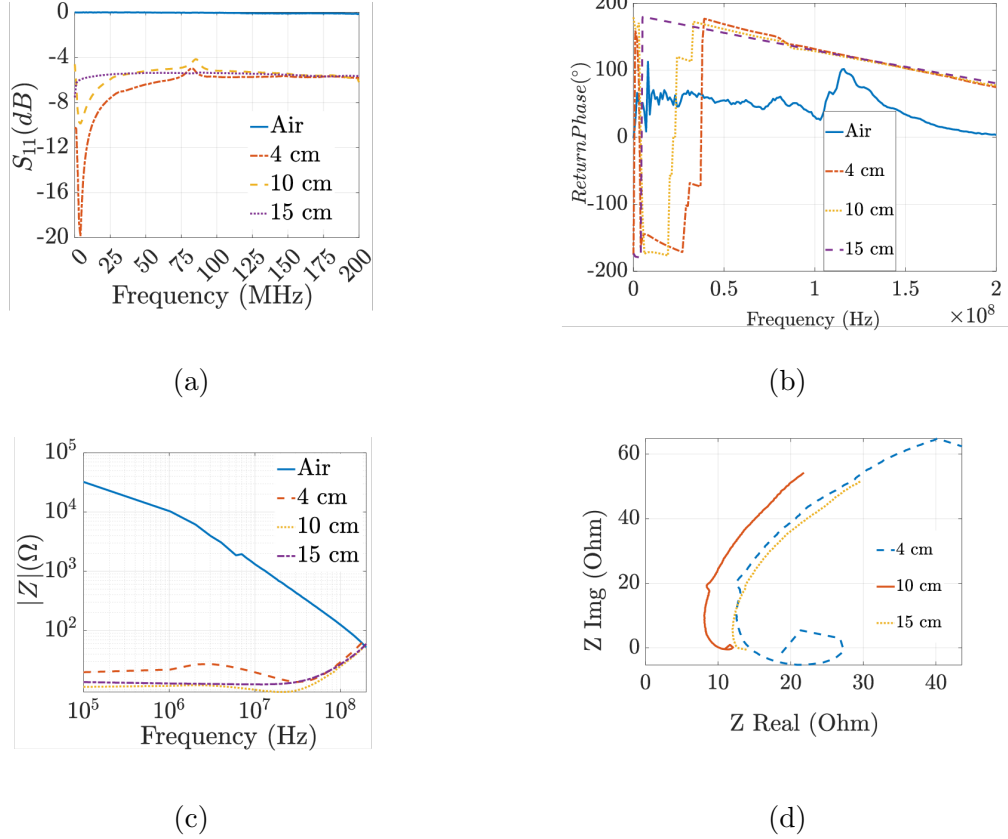


Figure 33: Planar Galvanic electrodes for different separations. Return Loss (S_{11}) (a), Return Phase (b), Impedance modulus $|Z|$ (c) and Nyquist Plot (d)

5.2. Discussions

According to [65], the dimensions of GE has most direct impact on GE coupling and return loss. In his study they use four shapes to show the impact on path loss: square, triangle, hexagon and circle. As conclusion of his studies they notice that the GE with more sides will result in a large coupling capacitance to the external ground, the circle and square result in more large attenuation and the triangle one has the most large attenuation. The results of my study shown that the attenuation for the circular and square electrodes is high with a minimum gap of difference between them. Besides the study of [65], show that the path loss increase with the distance which is proved in our studies and the effects of the angle were studied by building the planar capacitive circle electrode. That indicated that the angle has a slightly effecting the return loss, with the planar capacitive electrode the return loss is more constant during whole range of

frequency.

We analyzed the impedance modules of the electrodes using the solution and three different distances. The $|Z|$ of the capacitive electrodes (Fig.30c and Fig.31c) present a peak at frequencies, similar to the Bode diagram of a series RLC circuit. It is also noticeable that for frequencies higher than the resonance peak of the capacitive electrodes the impedance in open (that means, air as the medium between electrodes) has values similar to the ones measured on the sodium chloride solution. We interpret that when the frequency is high enough, the most beneficial path for the electromagnetic wave is jumping directly from the skin electrode to the same ground electrode without flowing through the medium. Contrariwise, the galvanic electrodes seem to have a pure inductive bode diagram, as shown in Fig.33c.

Based on the previous results see in Table.8. We decided to focus on using the circular capacitive electrodes.

Table 8: Measurements of electrodes with VNA

Type of electrodes	Square electrodes	Circular electrodes	Circular Plannar electrodes	Galvanic electrodes
High transmission peak	-12 dB at 4cm in 100 Mhz	-20 dB at 4cm in 100 Mhz	-15 dB at 10cm in 20Mhz	-25 at 15 cm in 25Mhz
Signal Delay	(+)phase<27 Mhz <(-)phase	(+)phase<20 Mhz<(-)phase	1Mhz<(-)phase> 10Mhz	(-)phase<50 Mhz<(+) phase
Higher Contact Impedance Peak	500 Ohms at 10cm	1000 Ohms at 15 cm	100 Ohms at 15cm	100 Ohms at 4cm
Nyquist Plot	Inductive Behavior <27Mhz < Capacitive behavior	Inductive Behavior <25Mhz < Capacitive behavior	Capacitive behavior <25Mhz < Inductive Behavior	Capacitive behavior <24Mhz <Inductive Behavior

5.3. Results of Transmission data through mediums

Circular capacitive electrodes were used on 3 mediums: salty water, gelatin and human arm to take into account propagation and contact impedance between the different mediums and electrodes see in Fig 34.

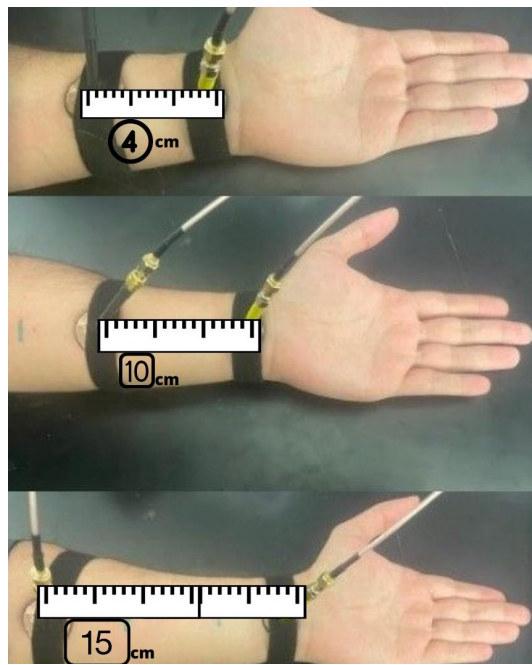
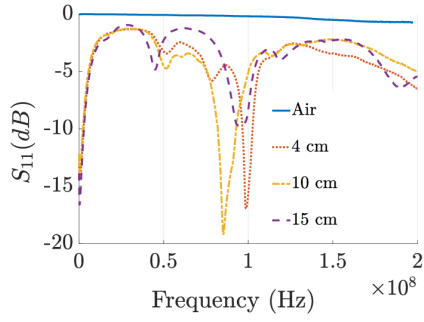


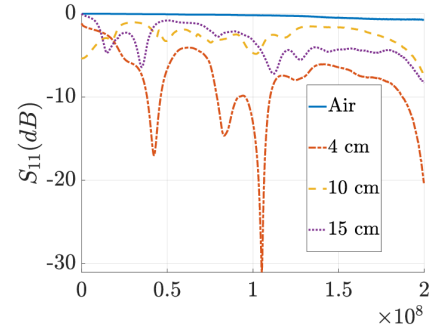
Figure 34: Experimental characterization of circular electrodes through Human Arm

5.3.1. Return Loss

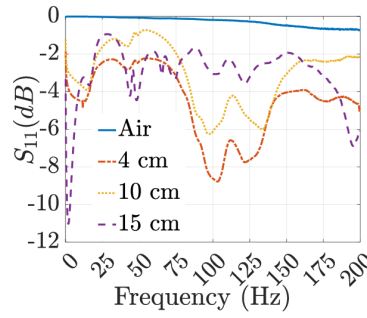
Fig. 35a shows a high peak around 80MHz and 100MHz at 4 and 10 cm but at 15 cm there is not a big loss over 10 dB in liquid samples. In Fig. 35b, gel samples show at 4 cm there was a good transmission around 10 to 30 db. However at 10 and 15 cm the reflection loss not over 5 dB. Fig. 35c, through the skin, the transmission loss do not over 10 db with all the distances and there are one peak of transmission at 100MHz.



(a)



(b)

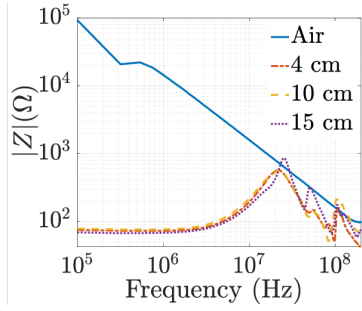


(c)

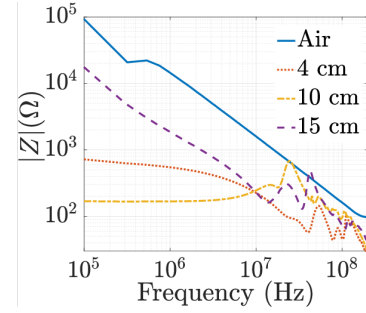
Figure 35: Channel characterization of the CC circular electrodes with axial excitation for different distances and media. Liquid medium return loss (a), Gel medium return loss (b) and measurement on subject's arm of the return loss (c)

5.3.2. Impedance

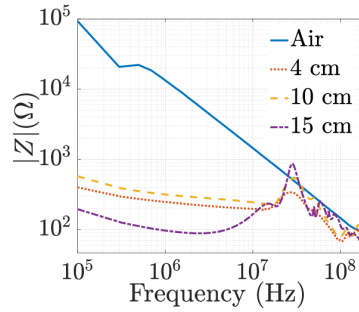
An impedance of no more than 1000 ohms is observed in all media, regardless of the distance between the electrodes. However, in the liquid medium the impedance increases beyond 1000 Mhz see in Fig 36a. In the case of Fig 36b. and Fig 36c. the highest impedance start from 100 kHz.



(a)



(b)



(c)

Figure 36: Channel characterization of the CC circular electrodes with axial excitation for different distances and media. Liquid medium of $|Z|$ (a), Gel medium of $|Z|$ (b), and measurement on subject's arm of $|Z|$ (c)

5.3.3. SWR

Standing Wave Ratio (SWR) is a function of the reflection coefficient, which describes the power reflected from the medium. The minimum VSWR is 1.0. In this case, no power is reflected from the antenna, which is ideal.

The VSWR specifications in Fig. 37a for a liquid medium are defined by:

1. $SWR < 3.0$ for $800 \text{ MHz} < f < 110\text{MHz}$ for 4, 10 and 15 cm.
2. $3.0 < SWR < 5.0$ for $180\text{MHz} < f < 200\text{MHz}$ for 4, 10 and 15 cm.
3. $5.0 < SWR < 10$ for $130\text{MHz} < f < 160\text{MHz}$ for 4, 10 and 15 cm.
4. $SWR > 10.0$ for $200 \text{ kHz} < f < 500 \text{ Khz}$ for 4, 10 and 15 cm.

In Fig. 37a , Specification numbers 1 and 2 reflected the least amount of SWR in a liquid medium regardless of the distance between Receiver and Transmitter electrode.

The VSWR specifications in Fig. 37b for a Gelatin medium are defined by:

1. $SWR < 3.0$ for $700 \text{ MHz} < f < 200\text{MHz}$ for 4cm .
2. $3.0 < SWR < 5.0$ for $120\text{MHz} < f < 200\text{MHz}$ for 15 cm.
3. $5.0 < SWR < 10$ for $800\text{KHz} < f < 100\text{MHz}$ for 10 and 15 cm.
4. $SWR > 10.0$ for $300 \text{ kHz} < f < 700 \text{ KHz}$ for 10 and 15 cm.

In Fig. 37b , Specification numbers 1 present least amount of SWR in a gelatin medium for 4 cm between Receiver and Transmitter electrode. Besides we observed a lot of fluctuations between an SWR between of 5 and 10 a long all frequency band.

The VSWR specifications in Fig. 37c in a Human Arm are defined by:

1. $SWR < 3.0$ no frequency between 100KHz and 200MHz for 4, 10 and 15 cm.
2. $3.0 < SWR < 5.0$ for 120MHz for 4 and 10 cm.
3. $5.0 < SWR < 10$ for $160\text{MHz} < f < 180\text{MHz}$ for 4,10 and 15 cm.
4. $SWR > 10.0$ for $300 \text{ kHz} < f < 800 \text{ KHz}$ for 10 and 15 cm respectively.

In Fig. 37c, Specification numbers 2 indicates the low value of SWR for 10 and 15 cm. Besides we observed that a lot of fluctuations between an SWR between of 4,10 and 15cm a long all frequency band.

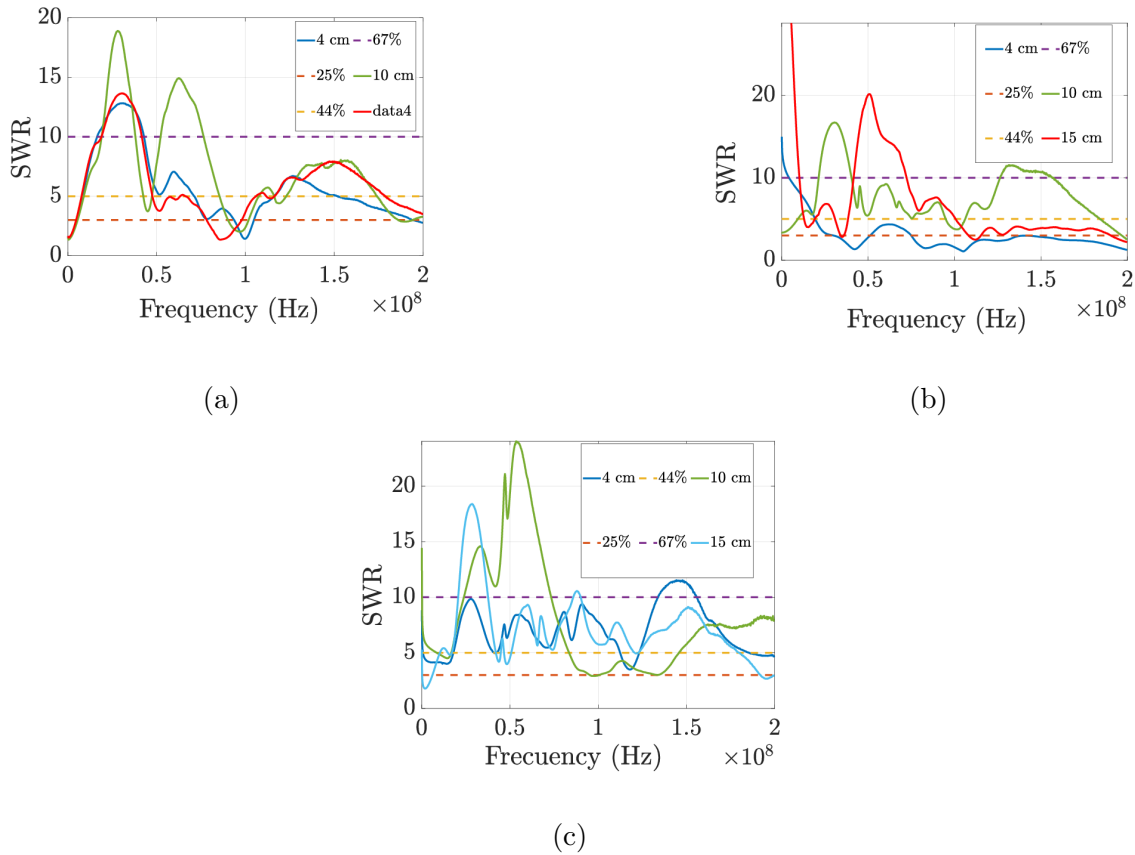


Figure 37: Channel characterization of the CC circular electrodes with axial excitation for different distances and media. Liquid medium of SWR (a), Gel medium of SWR (b), and measurement on subject's arm of SWR (c)

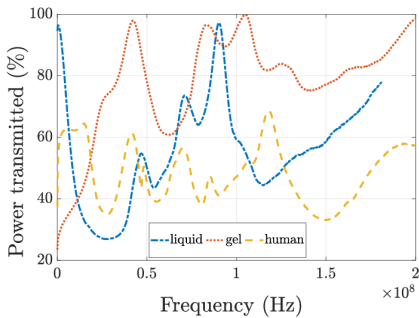
5.3.4. Power Transmitted

Fig. 38a shows the Percentage of the power transmitted from Tx electrode to the Rx receptor with a distance of 4 cm between them in our 3 mediums: liquid, gel and human arm. We can see that over 70KHz there is a good transmission between 70% to 90%. In the case of human arm, there is transmission less that 70% during all the frequency band.

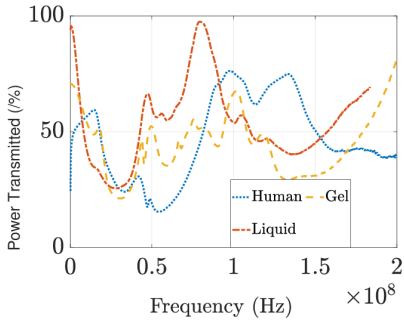
Fig. 38b shows the Percentage of the power transmitted from Tx electrode to the Rx receptor with a distance of 10 cm between them in our 3 mediums: liquid, gel and human arm. We can see that around 100MHz there is a good transmission over 50% in the three mediums. In the case of human arm, there is transmission less that 70%

during all the frequency band.

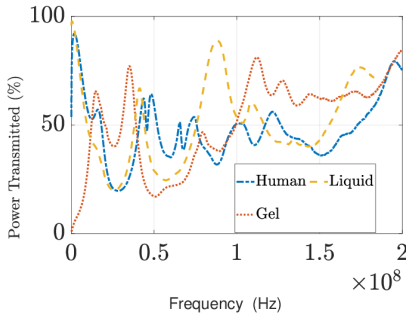
Fig. 38c shows the Percentage of the power transmitted from Tx electrode to the Rx receptor with a distance of 15 cm between them in our 3 mediums: liquid, gel and human arm. We can see that in liquid a gel medium with a frequency higher of 100 MHz there is there is piks of more of 50%.In the case of human arm, there is transmission less that 50% during all the frequency band.



(a)



(b)



(c)

Figure 38: Channel characterization of the CC circular electrodes with axial excitation for different distances and media. Liquid medium of % Power Transmitted (a), Gel medium of % of Power Transmitted (b), and measurement on subject's arm of % of Power Transmitted (c)

5.4. Discussions

Table 9 summarizes the results obtained for the MiniVNA Pro, the transmission peaks were large at shorter distances in the case of decreasing impedance with increasing frequency without exceeding 1000 Ohms and the Nyquist plot shows an inductive behavior at low frequencies and capacitive behavior at high frequencies. [66] suggests frequencies below 82 Mhz for the IBC technique. Our results show the highest transmission peak at 100 Mhz. However it does not exceed -8dB.

In the case of the circular capacitive electrode. We observed that the channel loss is primarily determined by the return path capacitance, which makes it independent of transmitter-receiver distance. However, the signal is influenced by external interference . [61] The interface's impedance can also attract external interferences and add unwanted noise to the biopotential. The studies of Kurian Polachan show that specific to HBC, the interface impedance can cause attenuation of the transmitted signals, limiting the received signal strength and thus restricting the bitrate of communication. As Electrode configuration, i.e., the placement of the electrode on the body, its parasitics to the earth's ground, and nearby objects, can also affect communication signal quality. [67]

Because the human body is a lossy dielectric medium, an attenuated voltage will be induced on the receiver load. The voltage signal experiences a change in its amplitude and phase due to the capacitive loss associated with the components of the human body. [68]. For this reason we observed a good signal transmission in a liquid medium which has better conductivity properties over the others mediums.

Often in the industry, antennas are screened (pass/fail criteria) based on VSWR specifications (VSWR specs). This is a method of measuring the antennas passively to determine if they are properly tuned in a quick manner. The antenna is measured with a network analyzer, and the VSWR as a function of frequency is recorded. We used the same method with our electrode and mediums

Table 9: Measurements of electrodes with VNA in diferents mediums

Type of medium	Salty Water	Gelatin	Human Arm
High transmiss- sion peak	-20 dB at 4cm	-30 dB at 4cm	-10 dB at 10cm
Higher Contact Impedance Peak	1000 Ohms	1000 Ohms	1000 Ohms
Nyquist Plot	Inductive Behavior <25Mhz < Capacitive behavior	Capacitive behavior in all frequency range	Inductive Behavior <20Mhz < Capacitive behavior

The parameter SWR is a measure that numerically describes how well the Rx electrode is impedance matched to the Tx electrode or transmission line it is connected to. In general, if the SWR is under 2 the electrodes match is considered ideal and little would be gained by impedance matching. As the SWR increases is obvious: that more power is reflected from the Tx electrode and therefore not transmitted [69].

We'll try to put the SWR number in context. Below Table 4 showing the relationship between SWR and total reflected power. Our results show three possible scenarios:

- SWR = 3 that means that 25% of the power is reflected.
- SWR = 5 that means that 44% of the power is reflected.
- SWR = 10 that means that 67% of the power is reflected.

Based on that we can notice that around 100Mhz we have less loss of power so we got a high percentage of signal transmitted and this is reflected in our Fig 38.

6. Conclusions

We investigated the effects of capacitance and the galvanic electrode through extensive analysis and actual measurements.

Our investigation reveals that the optimal signal transmission frequency is around 100 MHz for capacitive coupling and for galvanic coupling it is less than 30 kHz regardless of the distance at which the signal is present. The second is the contact impedance between the electrodes. increases when the distance between them increases regardless of the type of electrodes.

Besides, Impedance is greater in a square shape over a circular shape. The planar excitation has a higher impedance than the axial one and the galvanic configuration showed several calibration errors and contact with the medium, so the values are not useful for comparison.

Finally, the highest impedance was found in the human arm, then in the gelatin, as the most conductive medium, water with salt was maintained with low impedance until to 100 MHz.

7. Future Perspectives

- As future research we will test in other mediums with properties of conductivity and permeability more precise like the human body phantoms.
- We will development a belt to have a better contact between the electrodes and the skin.
- We also will investigate separately the effect of temperature, dry and wet skin, and other factors on the received signal in real experiments.
- We plan to use the N9914B RF Fieldfox and development more deeply our software to create a safety database of our experiments on humans.

8. References

References

- [1] C. Gabriel, E. Grant, R. Tata, P. Brown, B. Gestblom, and E. Noreland, "Microwave absorption in aqueous solutions of dna," *Nature*, vol. 328, no. 6126, pp. 145–146, 1987.
- [2] X.-F. Teng, Y.-T. Zhang, C. C. Poon, and P. Bonato, "Wearable medical systems for p-health," *IEEE reviews in Biomedical engineering*, vol. 1, pp. 62–74, 2008.
- [3] C. D. Mathers and D. Loncar, "Projections of global mortality and burden of disease from 2002 to 2030," *PLoS medicine*, vol. 3, no. 11, p. e442, 2006.
- [4] W. H. Organization, P. H. A. of Canada, C. P. H. A. of Canada *et al.*, *Preventing chronic diseases: a vital investment*. World Health Organization, 2005.
- [5] C.-M. Tang and R. Bashirullah, "Channel characterization for galvanic coupled in vivo biomedical devices," in *2011 IEEE International Symposium of Circuits and Systems (ISCAS)*. IEEE, 2011, pp. 921–924.
- [6] M. Scholtz, "Addressing the global demands for improved healthcare," *Proc. Telemedicine 21st Century, Opportunities Citizens, Society, Industry*, pp. 11–18, 1999.
- [7] A. Lymberis, "Smart wearable systems for personalised health management: Current r&d and future challenges," in *Proceedings of the 25th annual International conference of the IEEE engineering in medicine and biology society (IEEE cat. No. 03CH37439)*, vol. 4. IEEE, 2003, pp. 3716–3719.
- [8] G. Tröster, "The agenda of wearable healthcare," *Yearbook of medical informatics*, vol. 14, no. 01, pp. 125–138, 2005.
- [9] J. E. Mezzich, "Psychiatry for the person: articulating medicine's science and humanism," *World Psychiatry*, vol. 6, no. 2, p. 65, 2007.

- [10] P. Bonato, “Wearable sensors/systems and their impact on biomedical engineering,” *IEEE Engineering in medicine and biology magazine*, vol. 22, no. 3, pp. 18–20, 2003.
- [11] L. Gatzoulis and I. Iakovidis, “Wearable and portable ehealth systems,” *IEEE Engineering in Medicine and Biology Magazine*, vol. 26, no. 5, pp. 51–56, 2007.
- [12] M. de Salud Publica, “Encuesta steps ecuador 2018: Vigilancia de enfermedades no transmitibles y factores de riesgo.”
- [13] J. Petäjäjärvi, K. Mikhaylov, R. Vuotoniemi, H. Karvonen, and J. Iinatti, “On the human body communications: wake-up receiver design and channel characterization,” *EURASIP Journal on Wireless Communications and Networking*, vol. 2016, no. 1, pp. 1–17, 2016.
- [14] K. Fujii, M. Takahashi, and K. Ito, “Electric field distributions of wearable devices using the human body as a transmission channel,” *IEEE transactions on Antennas and Propagation*, vol. 55, no. 7, pp. 2080–2087, 2007.
- [15] M. A. Callejon, J. Reina-Tosina, D. Naranjo-Hernández, and L. M. Roa, “Galvanic coupling transmission in intrabody communication: A finite element approach,” *IEEE Transactions on Biomedical Engineering*, vol. 61, no. 3, pp. 775–783, 2013.
- [16] J. F. Zhao, X. M. Chen, B. D. Liang, and Q. X. Chen, “A review on human body communication: Signal propagation model, communication performance, and experimental issues,” *Wireless Communications and Mobile Computing*, vol. 2017, 2017.
- [17] J. A. Ruiz, J. Xu, and S. Shimamoto, “Propagation characteristics of intra-body communications for body area networks,” in *CCNC 2006. 2006 3rd IEEE Consumer Communications and Networking Conference, 2006.*, vol. 1. Citeseer, 2006, pp. 509–513.
- [18] R. Kumar and R. Mukesh, “State of the art: Security in wireless body area networks,” *International Journal of Computer Science & Engineering Technology (IJCSSET)*, vol. 4, no. 05, pp. 622–630, 2013.

- [19] S. Al-Janabi, I. Al-Shourbaji, M. Shojafar, and S. Shamshirband, "Survey of main challenges (security and privacy) in wireless body area networks for healthcare applications," *Egyptian Informatics Journal*, vol. 18, no. 2, pp. 113–122, 2017.
- [20] A. Fragopoulos, J. Gialelis, and D. Serpanos, "Imposing holistic privacy and data security on person centric ehealth monitoring infrastructures," in *The 12th IEEE International Conference on e-Health Networking, Applications and Services*. IEEE, 2010, pp. 127–134.
- [21] H. Taleb, A. Nasser, G. Andrieux, N. Charara, and E. Motta Cruz, "Wireless technologies, medical applications and future challenges in wban: a survey," *Wireless Networks*, vol. 27, no. 8, pp. 5271–5295, 2021.
- [22] J. Wang, Z. Zhang, K. Xu, Y. Yin, and P. Guo, "A research on security and privacy issues for patient related data in medical organization system," *International Journal of Security and Its Applications*, vol. 7, no. 4, pp. 287–298, 2013.
- [23] Y. Niu, S. Nazeri, W. Hashim, A. A. A. Alkahtani, H. R. Abdulshaheed *et al.*, "A survey on short-range wban communication; technical overview of several standard wireless technologies," *Periodicals of Engineering and Natural Sciences*, vol. 9, no. 4, pp. 877–885, 2021.
- [24] K. Hasan, K. Biswas, K. Ahmed, N. S. Nafi, and M. S. Islam, "A comprehensive review of wireless body area network," *Journal of Network and Computer Applications*, vol. 143, pp. 178–198, 2019.
- [25] H. R. Abdulshaheed, Z. T. Yaseen, A. M. Salman, and I. Al-Barazanchi, "A survey on the use of wimax and wi-fi on vehicular ad-hoc networks (vanets)," in *IOP Conference Series: Materials Science and Engineering*, vol. 870, no. 1. IOP Publishing, 2020, p. 012122.
- [26] J. D. Taylor, "Ultra-wideband radar overview," in *Introduction to ultra-wideband radar systems*. CRC Press, 2020, pp. 1–10.
- [27] I. Al Barazanchi, H. R. Abdulshaheed, and A. Shibghatullah, "The communication technologies in wban," *Int. J. Adv. Sci. Technol*, vol. 28, no. 8, pp. 543–549, 2019.

- [28] R. A. Khan and A.-S. K. Pathan, “The state-of-the-art wireless body area sensor networks: A survey,” *International Journal of Distributed Sensor Networks*, vol. 14, no. 4, p. 1550147718768994, 2018.
- [29] Y. Qu, G. Zheng, H. Ma, X. Wang, B. Ji, and H. Wu, “A survey of routing protocols in wban for healthcare applications,” *Sensors*, vol. 19, no. 7, p. 1638, 2019.
- [30] E. P. Balogh, B. T. Miller, and J. R. Ball, “Improving diagnosis in health care,” 2015.
- [31] T. Wu, F. Wu, J.-M. Redoute, and M. R. Yuce, “An autonomous wireless body area network implementation towards iot connected healthcare applications,” *IEEE access*, vol. 5, pp. 11 413–11 422, 2017.
- [32] R. Contreras, M. Huerta, G. Sagbay, C. LLumiguan, M. Bravo, A. Bermeo, R. Clotet, and A. Soto, “Tremors quantification in parkinson patients using smart-watches,” in *2016 IEEE Ecuador Technical Chapters Meeting (ETCM)*. IEEE, 2016, pp. 1–6.
- [33] Z. Dong, H. Gu, Y. Wan, W. Zhuang, R. Rojas-Cessa, and E. Rabin, “Wireless body area sensor network for posture and gait monitoring of individuals with parkinson’s disease,” in *2015 IEEE 12th International Conference on Networking, Sensing and Control*. IEEE, 2015, pp. 81–86.
- [34] G. M. Abdulsahib and O. I. Khalaf, “Comparison and evaluation of cloud processing models in cloud-based networks,” *International Journal of Simulation–Systems, Science & Technology*, vol. 19, no. 5, p. 64, 2018.
- [35] M. W. Alam, T. Sultana, and M. S. Alam, “A heartbeat and temperature measuring system for remote health monitoring using wireless body area network,” *International Journal of Bio-Science and Bio-Technology*, vol. 8, no. 1, pp. 171–190, 2016.
- [36] K. Abualsaud, M. Mahmuddin, M. Saleh, and A. Mohamed, “Ensemble classifier for epileptic seizure detection for imperfect eeg data,” *The Scientific World Journal*, vol. 2015, 2015.

- [37] A. Pal, “Sensor based computational model to control the spreading of covid-19 virus in a smart city,” *Studies in Indian Place Names*, vol. 40, no. 70, pp. 4983–4994, 2020.
- [38] D. McIlwraith and G.-Z. Yang, “Body sensor networks for sport, wellbeing and health,” in *Sensor Networks*. Springer, 2010, pp. 349–381.
- [39] A. Asif and I. A. Sumra, “Applications of wireless body area network (wban): A survey,” *Engineering science and technology international research journal*, pp. 64–71, 2017.
- [40] D. Naranjo-Hernández, A. Callejón-Leblic, Ž. Lučev Vasić, M. Seyedi, and Y.-M. Gao, “Past results, present trends, and future challenges in intrabody communication,” *Wireless communications and mobile computing*, vol. 2018, 2018.
- [41] X. Lai, Q. Liu, X. Wei, W. Wang, G. Zhou, and G. Han, “A survey of body sensor networks,” *Sensors*, vol. 13, no. 5, pp. 5406–5447, 2013.
- [42] I. Čuljak, Ž. Lučev Vasić, H. Mihaldinec, and H. Džapo, “Wireless body sensor communication systems based on uwb and ibc technologies: State-of-the-art and open challenges,” *Sensors*, vol. 20, no. 12, p. 3587, 2020.
- [43] J. Mao, H. Yang, Y. Lian, and B. Zhao, “A self-adaptive capacitive compensation technique for body channel communication,” *IEEE transactions on biomedical circuits and systems*, vol. 11, no. 5, pp. 1001–1012, 2017.
- [44] I. C. on Non-Ionizing Radiation Protection *et al.*, “Guidelines for limiting exposure to electromagnetic fields (100 khz to 300 ghz),” *Health physics*, vol. 118, no. 5, pp. 483–524, 2020.
- [45] S. Maity, M. Nath, G. Bhattacharya, B. Chatterjee, and S. Sen, “On the safety of human body communication,” *IEEE Transactions on Biomedical Engineering*, vol. 67, no. 12, pp. 3392–3402, 2020.
- [46] D. Andreuccetti, “An internet resource for the calculation of the dielectric properties of body tissues in the frequency range 10 hz-100 ghz,” <http://niremf.ifac.cnr.it/tissprop/>, 2012.

- [47] C. Gabriel, "Compilation of the dielectric properties of body tissues at rf and microwave frequencies." King's Coll London (United Kingdom) Dept of Physics, Tech. Rep., 1996.
- [48] D. M. Pozar, *Microwave engineering*. John wiley & sons, 2011.
- [49] J. C. Maxwell, *A dynamical theory of the electromagnetic field*. Wipf and Stock Publishers, 1996.
- [50] M. S. Wegmueller, M. Oberle, N. Felber, N. Kuster, and W. Fichtner, "Signal transmission by galvanic coupling through the human body," *IEEE Transactions on Instrumentation and Measurement*, vol. 59, no. 4, pp. 963–969, 2009.
- [51] D. Muramatsu, F. Koshiji, K. Koshiji, and K. Sasaki, "Input impedance analysis of a human body communication transmitter using a realistic human model and a simplified layered model," *Journal of Japan Institute of Electronics Packaging*, vol. 16, no. 7, pp. 528–534, 2013.
- [52] Ž. Lucev, I. Krois, and M. Cifrek, "A capacitive intrabody communication channel from 100 khz to 100 mhz," *IEEE Transactions on Instrumentation and Measurement*, vol. 61, no. 12, pp. 3280–3289, 2012.
- [53] M. D. Pereira, G. A. Alvarez-Botero, and F. R. de Sousa, "Characterization and modeling of the capacitive hbc channel," *IEEE Transactions on Instrumentation and Measurement*, vol. 64, no. 10, pp. 2626–2635, 2015.
- [54] Y. M. Chi, T.-P. Jung, and G. Cauwenberghs, "Dry-contact and noncontact biopotential electrodes: Methodological review," *IEEE reviews in biomedical engineering*, vol. 3, pp. 106–119, 2010.
- [55] M. D. Pereira, K. T. Silvestri, and F. R. de Sousa, "Measurement results and analysis on a hbc channel," in *2014 IEEE International Symposium on Medical Measurements and Applications (MeMeA)*. IEEE, 2014, pp. 1–6.
- [56] K. Hachisuka, T. Takeda, Y. Terauchi, K. Sasaki, H. Hosaka, and K. Ito, "Intrabody data transmission for the personal area network," *Microsystem Technologies*, vol. 11, no. 8-10, pp. 1020–1027, 2005.

- [57] T. G. Zimmerman, J. R. Smith, J. A. Paradiso, D. Allport, and N. Gershenfeld, “Applying electric field sensing to human-computer interfaces,” in *Proceedings of the SIGCHI conference on Human factors in computing systems*, 1995, pp. 280–287.
- [58] M. Seyedi, Z. Cai, and D. T. Lai, “Characterization of signal propagation through limb joints for intrabody communication,” *International Journal of Biomaterials Research and Engineering (IJBRE)*, vol. 1, no. 2, pp. 1–12, 2011.
- [59] A. Celik and A. Eltawil, “The internet of bodies: The human body as an efficient and secure wireless channel.” Submitted to IEEE, 2021.
- [60] T. G. Zimmerman, “Personal area networks: Near-field intrabody communication,” *IBM systems Journal*, vol. 35, no. 3.4, pp. 609–617, 1996.
- [61] S. Maity, K. Mojabe, and S. Sen, “Characterization of human body forward path loss and variability effects in voltage-mode hbc,” *IEEE Microwave and Wireless Components Letters*, vol. 28, no. 3, pp. 266–268, 2018.
- [62] B. Adamczyk, *Foundations of Electromagnetic Compatibility: with Practical Applications*. John Wiley & Sons, 2017.
- [63] D. Häring and B. Adamczyk, “Smith chart use in rf design and emc testing,” 2019.
- [64] A. Pinto, P. Bertemes-Filho, and A. Paterno, “Gelatin: A skin phantom for bioimpedance spectroscopy,” *Biomedical Physics & Engineering Express*, vol. 1, no. 3, p. 035001, 2015.
- [65] J. Mao, B. Zhao, Y. Lian, and H. Yang, “The effects of gnd electrodes in capacitive-coupling body channel communication,” in *2015 IEEE Biomedical Circuits and Systems Conference (BioCAS)*. IEEE, 2015, pp. 1–4.
- [66] M. H. Seyedi and D. Lai, *A novel intrabody communication transceiver for biomedical applications*. Springer, 2017.
- [67] K. Polachan, B. Chatterjee, S. Weigand, and S. Sen, “Human body–electrode interfaces for wide-frequency sensing and communication: A review,” *Nanomaterials*, vol. 11, no. 8, p. 2152, 2021.

- [68] H. Elayan and R. M. Shubair, "On channel characterization in human body communication for medical monitoring systems," in *2016 17th International Symposium on Antenna Technology and Applied Electromagnetics (ANTEM)*. IEEE, 2016, pp. 1–2.
- [69] R. A. Shafik, M. S. Rahman, A. R. Islam, and N. S. Ashraf, "On the error vector magnitude as a performance metric and comparative analysis," in *2006 International Conference on Emerging Technologies*. IEEE, 2006, pp. 27–31.